The interaction of ICAM-1 with LFA-1: intercellular signaling and implication in type I diabetes

by

Courtney W. Gdowski

B.S., University of Kansas, 2008

Submitted to the Department of Molecular Biosciences
and the Faculty of the Graduate School of the University of Kansas
in partial fulfillment of the requirements for the
degree of Master of Arts

_____

Dr. Stephen H. Benedict,
Chair

_____

Dr. Tom Yankee

_____

Dr. Scott Hefty

Date Defended: April 12th, 2012

The Thesis Committee for Courtney W. Gdowski

certifies that this is the approved version of the following thesis:

The interaction of ICAM-1 with LFA-1: intercellular signaling and implication in type I diabetes

_____

Chairperson, Dr. Steve Benedict

Date approved: April 12th, 2012

Abstract

T lymphocytes are cells that play an essential role in both the regulation and activation of an immune response. Proper regulation of T cell activation requires two costimulatory signals, one from the T cell receptor (TCR)-CD3 complex and the second from a surface molecule on an antigen presenting cell (APC). The first signal is characterized by the TCR-CD3 complex binding cognate antigen as it is being presented on a major histocompatibility complex (MHC) molecule. The second signal involves binding of a costimulatory molecule on the surface of a T cell with a counter receptor present on the surface of an APC.

ICAM-1, the focus of the present work, is a cell surface protein located on T cells and functions in adhesion and extravasation of the cell during inflammation. Our lab and others have previously published that ICAM-1 is also capable of receiving the second signal for T cell activation. In the present work, we elucidated the components of the signaling complex formed after stimulation through ICAM-1. The proteins identified thus far include mitogen- activated protein kinase (MAPK), cdc2 kinase, CD45, LFA-1, LAT, Gads, the Src tyrosine kinase family proteins Lck and Fyn, and the ZAP-70/CD3ζ complex.

Since the ICAM-1/LFA-1 interaction is essential for proper T cell function, blocking the interaction could be a useful means of regulating improper immune response and treating the diseases associated with its dysfunction. Previous studies in our lab using peptides to block the ICAM-1/LFA-1 interaction have proven beneficial in treating

several autoimmune diseases. Here we sought to test a shorter course of peptide therapy and evaluated the treatment in a model for type I diabetes. The peptides not only delayed the onset of diabetes in the treated animals, but also drastically reduced the amount of infiltration seen within the islets of the pancreas.

We also used computational approaches to develop an alternative set of peptides with an increased affinity for ICAM-1 and LFA-1 and assessed their effect on T cell activation and function. We found that both peptides were able to inhibit MDHC-induced T cell adhesion indicating specificity for both ICAM-1 and LFA-1. We also found that stimulating with anti-CD3 in the presence of each peptide caused a marked increase in proliferation of human T cells. This result suggests that the redesigned peptides are capable of acting as a costimulatory signal.

Dedication

I would like to dedicate this thesis to my husband, Mark, and my little man, Henry. You make up the best parts of my being and I thank God every day for my boys. You accept me for the person I was, love me for the person I am and celebrate the person I will become. I could not ask for a better family.

Acknowledgements

I would like to first and foremost thank my advisor, Dr. Steve Benedict. He has helped guide my career and fostered my scientific (and oftentimes offbeat) mind with a sense of humor. His hard work and constant belief in me made this thesis possible. I would also like to thank Dr. Marci Chan and Dr. Tom Yankee for their constant support and ideas to further each experiment. They listened tirelessly failed western blot after failed western blot and offered wonderful suggestions and words of encouragement. I would also like to thank Dr. Scott Hefty who was the first scientific mentor I ever had the pleasure of working with. He was the first to help excite me about the daily grind of bench top research and I will forever be grateful for letting me "get my feet wet" and perform my undergraduate research in his lab. The redesigned peptides would not have been possible without the help of Dr. John Karanicolas and Whitney Smith who both were instrumental in helping an immunology student learn computer code. The women of 7035, Abby Dotson, Amy Hinkelman and Kelli Williams will forever hold a special place in my heart. They truly made the lab feel like a family… and a fun one at that, with the veggie chili cook-offs, pencil games and capsid tennis.

I must thank my family. My parents, who still to this day have no idea what I do, supported me with every fiber of their beings. My dad still wonders when I will start working on "A" cells (since according to him cells are named alphabetically). My sister, who always made me smile even when I was falling down and my brother, who has always been there for me even when I didn't know I needed someone around. Finally, I want to thank my boys. My husband, Mark, was not only my sounding board for complaints, but also was an indispensible reference and guide. Without his support and love, I would probably be an unhappy medical student with too many shoes. As unconventional as it may be, I have to also thank our dog, Elle. She always knew exactly how to cheer me up when I had a bad day. And last, but certainly not least, the last thank you is reserved for the littlest person in my life, our son Henry. I didn't know how much I was missing until he came into my life and made me whole.

Table of Contents

Table of Contents

List of Figures and Tables

Chapter 1:

Introduction and Background Information

Introduction

The Immune System. The immune system forms the defense mechanism of a host against the outside world. It is comprised of a network of cells and small molecules capable of recognizing and responding to an array of perceived danger, such as antigens from pathogenic organisms and altered cells that can lead to cancer.

The human immune system is divided into two distinct branches: the innate immune system and the adaptive immune system. Together these two branches cover the spectrum of possible dangers a human could encounter and allow for an appropriate response to be mounted. Components from both systems constantly survey the host and once a foreign antigen is recognized, an immune response is initiated leading to elimination of the foreign agent.

Innate immunity is considered nonspecific; it functions in creating physiological and anatomical barriers that protect the host in response to any perceived threat. If a threat is found, an inflammatory response is initiated that causes vasodilation and increased vascular permeability to allow for nonspecific phagocytic cells, such as monocytes, macrophages and neutrophils, to enter the inflammatory milieu. The innate immune response is considered nonspecific in that it responds in the same way to all danger, whether it be a splinter or a bacterial infection.

The adaptive immune response is responsible for the specificity associated with immunity. This system recognizes and responds to specific foreign antigens present on organisms. The success of the adaptive response is predicated on the ability of the system to distinguish ‘self’ from ‘non-self’ and to create an amplified response to antigens

previously encountered allowing for immunological memory. Cells that participate in adaptive immunity include T lymphocytes (T cells), B lymphocytes (B cells) and antigen-presenting cells (APCs).

T cells. The cells that help to initiate the adaptive immune response to a foreign organism are T cells. T cells are named as such because they develop in the thymus. Although they originate in the bone marrow as thymic precursors, they eventually migrate to the thymus where they mature as thymocytes. Thymocytes express several cell surface proteins, including two essential proteins collectively termed the T cell receptor (TCR). Each TCR is capable of interacting with only one unique antigen (cognate antigen). The subunits of the TCR (α/β) are supported by a cluster of accessory proteins collectively termed the CD3 complex. The entire CD3 complex includes ζζ, γε and εδ dimers in additional to the α/β subunits of the TCR itself. These accessory proteins function for both stability and signal transduction.

The adaptive response is initiated upon binding of the T cell receptor (TCR)-CD3 protein complex to its cognate antigen present on the major histocompatibility complex (MHC) on the surface of an antigen-presenting cell. This signal coupled with a costimulatory signal (described below) lead to both T cell activation and secretion of soluble factors that activate other immune system components. This interaction between the TCR and cognate antigen provides both specificity and the first signal for T cell activation, however this signal alone is not enough to drive full activation. A second signal is also required to prevent the T cell from becoming anergic and provides the necessary co-stimulation required for differentiation. The second signal is also delivered

intercellularly between the T cell and the APC, however it does not require the presence of cognate antigen to occur. Once both signals have transpired, the T cell differentiates to an effector cell that secretes cytokines to direct further cell activation and mount an effective immune response.

The study of signaling through a cell surface receptor can be done *in vitro* through stimulation with an antibody specific for that molecule. Binding of the antibody to the receptor mimics the natural binding between a ligand and the receptor and can initiate signaling. Antibodies against CD3 have been widely used due to the ability of the antibody to induce signaling events normally associated with TCR engagement (1,2).

Costimulatory molecules. The traditional second signal protein present on a T cell, CD28, interacts with its counter receptor, B7, on the surface of an APC leading to clonal expansion, interleukin-2 (IL-2) secretion, and memory cell development. While CD28 has been the most well characterized signal, several other costimulatory molecules also have been identified including CD2, CD45, CD5 and the adhesion molecules LFA-1 and ICAM-1 (3-9).

The costimulatory molecule focused on in the present work, ICAM-1, can also act as the second signal comparable to CD28 and results in greater proliferation, greater protection from apoptosis and more T cells exhibiting a memory phenotype as compared to stimulation through LFA-1 (10-12). Upon ICAM-1 stimulation, generation of a Th1 subset is seen as well as induction of IL-2 transcription and secretion, expression of the activation marker CD69, and activation of phosphotidylinositol-3-kinase (PI3K) (11). Moreover, co-stimulation through ICAM-1 has been shown to initiate kinase activity as

well as inactivation of cdc2 kinase, suggesting the ICAM-1 also plays a role in cell cycle regulation (13).

Adhesion molecules. Adhesion molecules are cell surface proteins that mediate the binding of cells through receptor-ligand interactions. Adhesion molecules are essential to biological events such as migration of leukocytes, hematopoesis and activation (14,15). The two adhesion molecules focused on in the present work are leukocyte function associated antigen-1 (LFA-1 or CD11a) and intercellular adhesion molecule-1 (ICAM-1 or CD54).

Integrins. Integrins are cell surface proteins that serve to anchor intercellular interactions such as cell:cell contact, development and cell migration (14). Integrins are heterodimeric glycoproteins composed of an α and β subunit that are noncovalently linked. The integrins are divided into subfamilies based upon the β subunit. There are currently 18 α subunits identified and 8 β subunits that can form some 24 unique integrins through different combinations (16). While there are 8 different subfamilies of integrins, the focus of work is on LFA-1, a member of the β_2 integrin family.

β_2 integrins are expressed only on lymphocytes. There are 4 known α subunits that interact with the β_2 subunit (CD18) to form the integrins α_L/β_2 (LFA-1/CD11a), α_x/β_2 (CD18/CD11c), α_m/β_2 (MAC-1/CD11b), and α_D/β_2 (CD11d). The ligands of the β_2 integrins include the blood proteins heparin and fibrinogen, tissue-associated proteins such as PSCD1, GNBL2L1 and FHL2 and the adhesion molecules ICAM-1, ICAM-2, ICAM-3, ICAM-4 and ICAM-5 (17-21).

Leukocyte function associated antigen-1. LFA-1 is a β_2 integrin expressed on all leukocytes whose ligands include ICAM-1, ICAM-2, ICAM-3, ICAM-4 and ICAM-5 (22). Interactions between LFA-1 and a ligand are the result of both the level of expression and the affinity for each ligand. Although ICAM-1 is not normally expressed at high levels on the cellular surface, ICAM-1 expression is inducible (as described below) and has an increased affinity for LFA-1 over ICAM-2 and ICAM-3 (23). The affinity of LFA-1 for a ligand can be upregulated through TCR stimulation and can be induced by stimulation through ICAM-3 and by low-affinity binding of ICAM-1 (24-27).

LFA-1 is the major mediator of cell-cell interactions within the immune system and alternations in avidity and affinity for a ligand contributes to the interaction (23). In addition to the role LFA-1 plays in adhesion, LFA-1 also functions as a costimulatory molecule. Stimulation through LFA-1 using either ligand or antibodies against LFA-1 results in the hydrolysis of PIP_2 and stimulation of intracellular Ca^{2+} in lymphocytes as well as tryrosine phosphorylation of the signaling intermediate Vav (28, 29). Stimulation through LFA-1 also turns on important transcription factors such as NF-AT, AP-1 and NF-κB that aid in T cell proliferation (28, 30-32).

Immunoglobulins and intercellular adhesion molecule-1. ICAM-1 is a member of the immunoglobulin superfamily. Immunoglobulins are glycosylated transmembrane proteins that aid in adhesion and cell survival. ICAM-1, also termed CD54, exists as a monomer, however non-covalently dimerizes upon stimulation (33). The levels of ICAM-1 expression on cells vary; ICAM-1 is highly expressed on dendritic cells, but expressed at low levels on T cells (34, 35). However, ICAM-1 expression can be upregulated by

inflammatory cytokines such as IFN-γ and TNF-α (36).

ICAM-1/LFA-1 interaction. The ICAM-1/LFA-1 interaction is traditionally associated with extravasation, or migration of leukocytes from the bloodstream into a tissue during inflammation. This process is accomplished in four distinct steps: rolling, activation, adhesion and diapedesis (**Figure 1.1**). Rolling occurs when selectins of the surface of a leukocyte bind to several proteins on the surface of endothelial cells. This low-affinity interaction serves to slow the travelling cell enough so that the cell can respond to stimuli such as chemokines and slow down enough for a high-affinity interaction to occur. The high-affinity interaction allows for the activation and adhesion steps where the binding of chemokines induces a conformational change in LFA-1 on the leukocyte surface to the activated form. Activated LFA-1 then binds to ICAM-1 expressed on the endothelial cell surface thereby arresting the cell on the vessel wall. This complete arrest allows for transendothelial migration to then occur where the leukocyte undergoes cytoskeletal rearrangement to permit travel between two endothelial cells.

Blocking LFA-1/ICAM-1 as a therapy. Many therapies have been developed that act to block the costimulatory signal with varying degrees of success. The absence of the second signal causes the T cell to undergo anergy or become apoptotic and thus therapies directed at inhibiting an active T cell response often seek to exploit this observation (27). Several groups have used the blocking of costimulatory molecules and their counter receptors in prevention of allograft rejection, reducing the onset of rheumatoid arthritis and insulin-dependent diabetes in mice (37-40). Our lab has developed peptides that

block the costimulatory signals normally induced by the interaction between ICAM-1 and LFA-1 (**Figure 1.2**). This blockade prevents the second signal from occurring thus causing anergy or apoptosis of the T cell.

The thesis. The dynamic functions of ICAM-1 require extensive further characterization in order to fully elucidate its complex regulatory role. The focus of this study is to identify the proteins associated with ICAM-1 that form a signaling complex capable of intracellular signaling. The proteins that we have identified thus far as associated with ICAM-1 include mitogen- activated protein kinase (MAPK), CD45, LFA-1, LAT, Gads, cdc2, the Src tyrosine kinase family proteins Lck and Fyn, TCRβ and the ZAP-70/CD3ζ complex. Characterization of the ICAM-1 associated signaling complex can yield a deeper understanding of the immune response at the molecular level and possibly hold further implications in disease related therapy**.**

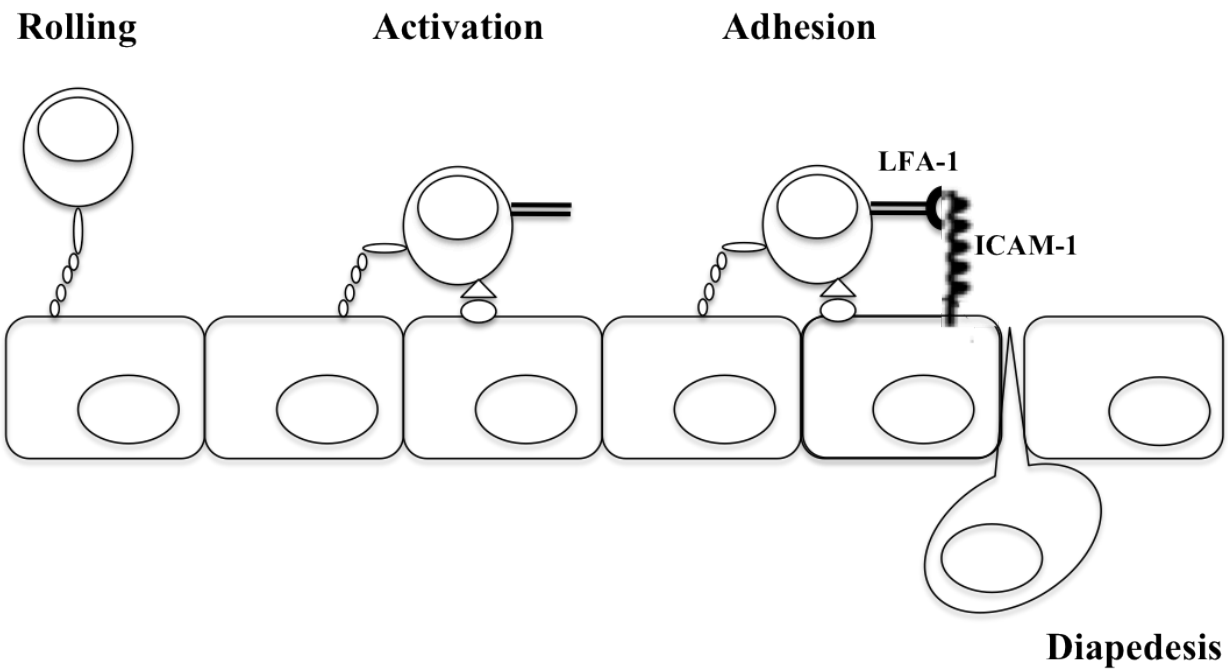
Rolling
Activation
Adhesion
LFA-1
ICAM-1
Diapedesis

Figure 1.1. Leukocyte Migration
The process of extravasation out of the bloodstream and into the tissues is mediated by the ICAM-1/LFA-1 interaction. The process is carried out in several steps, including (1) rolling along the vascular endothelium via selectins, (2) activation of integrins by stimulation with cytokine, (3) strong adhesion mediated by ICAM-1/LFA-1 and (4) transendothelial migration through the endothelial cell junctions.

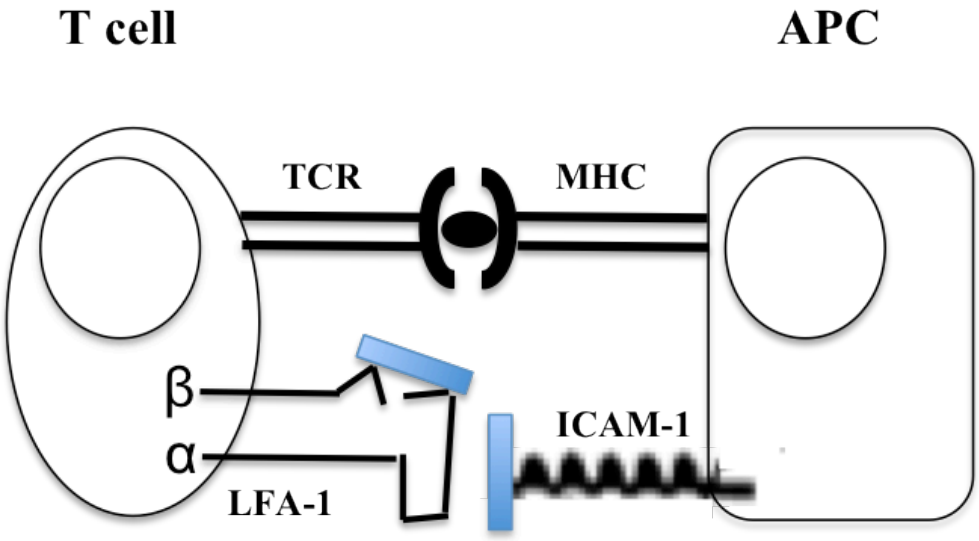
T cell
APC
TCR
MHC
β
α
LFA-1
ICAM-1

Figure 1.2. Schematic of the proposed function of the LFA-1 and ICAM-1-derived peptides
Peptides derived from the sequence located in the binding interface between ICAM-1 and LFA-1 have been shown to block the interaction. It is hypothesized that the peptides (blue) act to physically block the ICAM-1/LFA-1 interaction leading to anergy or apoptosis of the cell.

Chapter 2:

The ICAM-1 Signaling Complex

Introduction

The hallmark of T cell signaling is formation of an immunological synapse that leads to the stimulation of kinase activity and thus to induction of specific gene expression. In an inflammatory environment, ligand recognition in the form of cognate antigen causes the migrating T cell to arrest and form a stable contact with the antigen-presenting cell. The T cell then forms a mature synapse at the site of recognition by recruiting receptors and signaling molecules that participate in transduction of the signal into the T cell resulting in gene activation.

The synapse itself serves as a molecular scaffold bringing signaling molecules into close proximity to allow for direct interaction between kinases and their target proteins. The synapse can be subdivided into sections based on the location of molecules within the supramolecular activation cluster (SMAC). The central SMAC (cSMAC) is enriched with TCR-MHC complexes, kinases and costimulatory proteins. The peripheral SMAC (pSMAC) is where adhesion molecules are located that keep the T cell and APC in close contact and allow for prolonged engagement of TCR-MHC and other ligand-receptor interactions. The distal region of the synapse (dSMAC) contains large, bulky proteins that otherwise would interfere with protein-protein interactions of the smaller signaling molecules.

Lipid rafts mediate this T cell signaling event by recruiting and transferring signal transduction molecules to the site of TCR engagement and cluster within the site of the immunological synapse (41-43). The importance of lipid raft involvement in signaling is highlighted by the observation that dispersal of lipid rafts inhibits T cell activation (44).

Our lab has previously shown that ICAM-1 is capable of acting as a costimulatory molecule, induces association and activation of the signaling kinases MAPK (ERK1/ERK2), Lck, ZAP-70 and cdc2 and turns on both IL-2 and *c-fos* gene expression (**Figure 2.1**). Based on these data, we were interested in determining the components of the induced signaling complex upon stimulation through ICAM-1. The work presented in this chapter highlights the role that associated proteins play in ICAM-1-induced signaling and the potential role ICAM-1 may play in an inflammatory context. Information on specific proteins identified later in this chapter is provided below.

Gads. Gads (Grb2-related adaptor protein), like Grb2, is a small adaptor protein composed of one SH2 and two SH3 domains. Grb2 and some Grb-2 related proteins have been shown to interact with signaling proteins such as SLP-76 and Cbl suggesting that Grb2 and its related proteins may couple signaling through the TCR to distinct pathways (49,50). Like other Grb2-related proteins, the SH2 domain of Gads has been shown to interact *in vitro* with tyrosine-phosphorylated Shc, however the SH3 domain of Gads does not bind to any known SH3 domain targets of Grb2 (48, 51). Gads binds the T cell signaling proteins SLP-76 through the SH3 domain and the linker of activated T cells (LAT) through the SH2 domain (52).

LFA-1. LFA-1 (lymphocyte function-associated antigen 1) is an integrin that has traditionally been associated with adhesion and migration of leukocytes through the tight junctions between endothelial cells during extravasation into tissues and has been implicated as a costimulatory signal capable of inducing T cell proliferation (53).

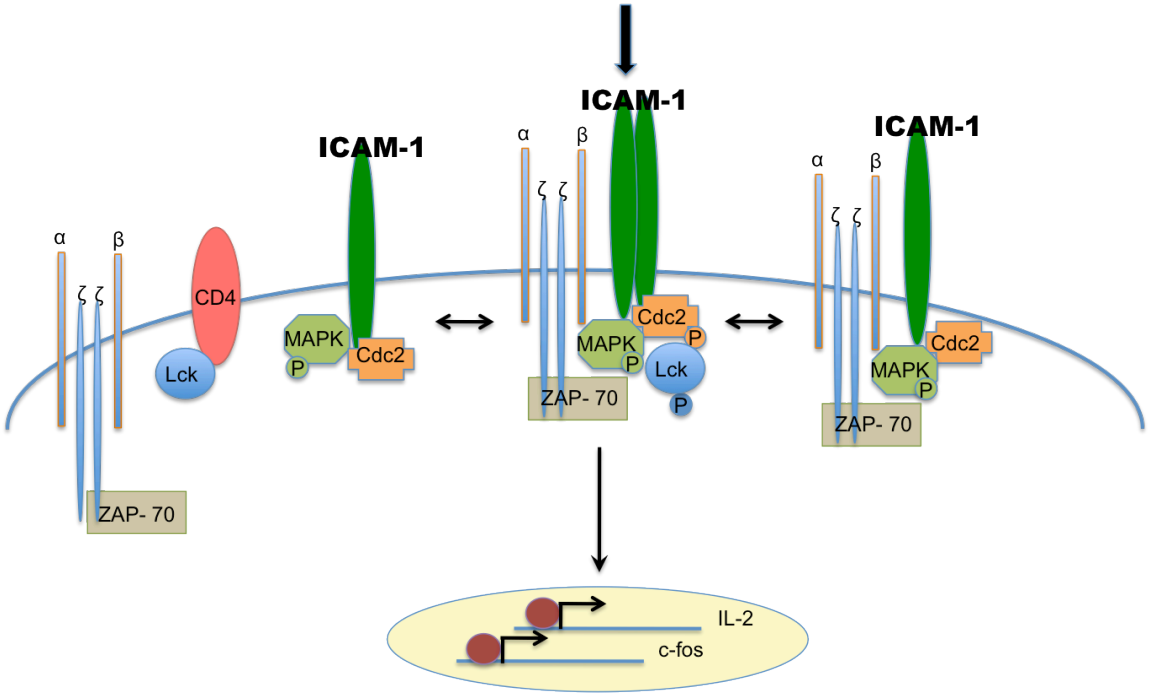
ICAM-1
ICAM-1
ICAM-1
α
β
ζ ζ
CD4
Lck
MAPK
P
Cdc2
Cdc2
P
MAPK
P
Lck
P
ZAP- 70
ZAP- 70
ZAP- 70
IL-2
c-fos

Figure 2.1. The associated kinases of the ICAM-1 signaling complex Previous studies completed by Dr. Chintana Chirathaworn and Br identified the association and activation of the kinases Lck, ERK1, ERK2 and cdc2 upon antibody stimulation through ICAM-1. ERK1 and ERK2 are constitutively associated and phosphorylated with ICAM-1 throughout the duration of the experiment. Lck is associated with ICAM-1 only after 2 minutes in the phosphorylated form and thereafter leaves the complex. cdc2 kinase is associated constitutively with ICAM-1, however the phosphorylated protein is only seen associated 2 minutes after stimulation.

In the context of signaling and the immunological synapse, LFA-1 mediates cell-cell interaction between the T cell and antigen-presenting cell (APC) by increasing adhesion through LFA-1 interaction with ICAM-1 on the surface of the APC. TCR signaling leads to a rapid increase of LFA-1-mediated adhesion through a conformational change in protein structure. This change to the active conformation of LFA-1 leads to increased avidity, clustering and affinity for ICAM-1 (54-56). LFA-1 is located in the peripheral ring (pSMAC) surrounding the cSMAC in the synapse where it functions as the major adhesion molecule involved in synapse formation and also acts to exclude CD45 from the synapse (57).

CD45. CD45 is a large protein tyrosine phosphatase that regulates both T and B cell receptor signaling. CD45 regulates T cell signaling through association with Src family kinases such as Lck and Fyn. The cytoplasmic tail of CD45 has intrinsic phosphatase activity and acts to remove inhibitory phosphate groups on Lck and Fyn and therefore plays a key role in initiation of T cell signaling.

Despite the major role CD45 plays in T cell activation, it can also inhibit protein-protein interactions necessary for successful T cell signaling events to occur due to its sheer size. LFA-1 acts to exclude CD45 from the synapse upon TCR engagement so that a successful signaling event can occur after CD45 has activated Lck and Fyn (57). If CD45 is left dispersed throughout the synapse, both the magnitude and duration of the TCR signal may be limited.

LAT. The linker for activated T cells (LAT) is small membrane-bound adaptor protein that is rapidly phosphorylated by ZAP-70 upon TCR engagement (58). Once activated, LAT acts as a scaffolding protein for SH2-domain containing molecules and recruits other signaling proteins to the synapse including Vav, PLCγ1, PI3K, Grb2, SLP-76, Gads and Cbl. The LAT knockout mouse, which shows a complete block in T cell development, perhaps best illustrates the importance of LAT involvement in signaling (59).

Fyn. Upon antigen recognition, the Src family kinases Lck and Fyn are activated and rapidly phosphorylate immunoreceptor tyrosine-based activation motifs (ITAMs) on the cytoplasmic tail of CD3ζ. This phosphorylation event allows for binding of the Src homology 2 (SH2) domain-containing protein ZAP-70 that subsequently is phosphorylated by Lck. Active Src-family kinases are able to phosphorylate downstream targets such as SLP-76 (45), Vav (46) and LAT (47) and are paramount in the initiation of signaling cascades involved in T cell activation and proliferation.

Immunoprecipitation and protein blotting studies were performed to identify the signaling complex that associates with ICAM-1 when peripheral T cells were stimulated through ICAM-1. These studies have identified several intracellular proteins involved in receptor-mediated lymphocyte activation in response to stimulation through ICAM-1. The signaling complex is fully formed between two and four minutes after stimulation and disassembly seen within 10 minutes. These results, coupled with specific kinase activity, suggest the mechanism by which ICAM-1 participates in T cell activation. The complex

identified thus far includes Src family kinases Lck and Fyn, CD3ζ, TCRβ, MAPK, cdc2, LFA-1, the CD45 isoforms CD45RA and CD45RB, and the adaptor proteins Gads and LAT.

Materials and Methods

Antibodies and reagents. Hybridomas expressing anti-CD54 (R6.5) and anti-CD11a (HB202) were purchased from ATCC (Manassas, VA) and antibodies were purified from serum-free medium using protein G affinity chromatography (Amersham). Anti-CD3 (OKT3) stimulating antibody was purchased from BD Biosciences. Anti-CD28 (ANC28.1) was purchased from Ancell. Anti-CD45, CD45RA and CD45RB were purchased from BioLegend. Anti-Fyn and LAT monoclonal antibodies were purchased from Epitomics. Anti-GADS was kindly provided by Dr. Tom Yankee. The cross-linking goat anti-mouse antibody was purchased from Biorad Laboratories. Biotinylated cholera toxin subunit B (Ctx-B) was purchased from Sigma (St. Louis, MO). Streptavidin-Cy3 was purchased from BioLegend.

Cell stimulation. Total T cells (20 x 10^6 cells/mL) were incubated at 37°C with 5 μg/mL of anti-ICAM-1. Goat anti-mouse IgG (2 μg/mL) was added 2 minutes later. Cells were lysed at indicated times in RIPA lysis buffer [10 mM Tris pH 8.0, 140 mM NaCl, 1% Triton X-100, 0.5% deoxycholate (DOC), 0.05% sodium dodecylsulfate (SDS), 100 mM NaF, 200 μM sodium orthovanadate, 1 mM phenylmethylsulfonylfluoride, 1 μg/mL leupeptide and 1 μg/mL pepstatin]. Lysed cells were incubated on ice for 30 minutes and centrifuged at 4°C at 11,000 rpm for 30 minutes. Supernatants were collected and protein concentrations were determined by Bradford Protein Assay (BioRad) per manufacturer's instructions. Lysates were stored at -70°C until used.

Immunoprecipitation and western blotting. Cell lysates were normalized to the lowest protein concentration prior to beginning the experiment. Pansorbin (Protein A-bearing *S. aureus*) was precoated with antibodies by incubating antibodies with Pansorbin for 1 hour at 4°C. Lysates were immunoprecipitated with antibody-coated Pansorbin overnight at 4°C. The resulting immune complexes were washed three times in RIPA buffer without DOC and SDS and once in RIPA buffer without any detergent (DOC, SDS or Triton X-100). Pellets were then resuspended in 2X SDS sample buffer [0.69 M Tris pH 6.6, 11% glycerol, 2.2% SDS, 0.71 M β-mercaptoethanol, and 0.028% bromophenol blue] and heated at 100°C for 5 minutes. Samples were then subjected to 10% SDS-PAGE.

SDS-PAGE gels were transferred to polyvinylidene fluoride (PVDF) membranes (Millipore) using a semi-dry electrophoretic transfer apparatus unit (Fisher Scientific) in transfer buffer [48 mM Tris, 39 mM Glycine pH 9.2, and 1.3 mM SDS] for 2 hours at 200 mA. Membranes were blocked using a commercial protein-free blocking buffer (Fisher Scientific) for 1 hour at room temperature with gentle agitation. Membranes were washed three times in Tris buffered saline plus Tween-20 (TBST) [50 mM Tris pH 7.0, 150 mM NaCl, and 0.1% Tween-20], incubated with indicated primary antibody for 1 hour at room temperature with gentle agitation and washed three times in TBST. Membranes were incubated with the appropriate secondary antibody for 1 hour, washed three times in TBST and incubated with commercial enhanced chemiluminescence reagent (GE, Amersham). The resulting blot was imaged using a Kodak Image Station 4000R imager to visualize protein bands.

For each identified protein within the complex, the reciprocal immunoprecipitation was also completed to verify the protein-protein interaction. For

example, since Gads was precipitated with anti-ICAM-1-coated Pansorbin, another immunoprecipitation was performed using anti-Gads-coated Pansorbin and probing the resulting blot for ICAM-1.

Fluorescence microscopy. Polystyrene microspheres (Polysciences, Inc.) were coated with anti-ICAM-1 (10 μg/ml), anti-ICAM+anti-CD3 (5 μg/ml), anti-CD28 (10 μg/ml)+anti-CD3 or mouse IgG1 isotype control overnight. Beads were washed in PBS to remove unbound antibody and resuspended at the concentration of 2×10^7 beads/ml. Jurkat T cells were stained with biotinylated-CtxB for 30 minutes at 37°C, washed twice in PBS and fixed using 3.7% paraformaldehyde. Fixed cells were mixed with antibody-coated beads at a 1:1 T cell:bead ratio and incubated 5 minutes at 37°C. Cells were stained with streptavidin-Cy3 for 30 minutes at 37°C, washed twice in PBS and deposited onto poly-L-lysine coated slides for 30 minutes at room temperature. Slides were treated with SlowFade (Molecular Probes) and stored at 4°C until analysis. Differential interference contrast (DIC) and fluorescence images were acquired using a Zeiss Axioplan microscope at 40X magnification.

Statistical analysis. Statistical analysis was performed using GraphPad Prism (GraphPad Software).

Results

Gads associates with ICAM-1 following stimulation of T cells through ICAM-1. As shown in **Figure 2.2**, immunoblotting was performed as described in the *Materials and Methods* in an attempt to identify an adaptor protein present in the ICAM-1 induced signaling complex. After extensive testing of candidate proteins, we were able to identify Gads as being constitutively associated with ICAM-1. **Table 1** lists all proteins tested and found to not be associated with the complex. Preliminary data also indicate that Gads may be inducibly associated with ICAM-1, with maximal association 2 minutes after stimulation through ICAM-1 (data not shown).

LAT associates with ICAM-1 following stimulation of T cells through ICAM-1. As shown in **Figure 2.3**, immunoblotting was performed as described previously and resulting blots were probed with anti-LAT. Similar to the association of adaptor protein, Gads (**Figure 2.2**), LAT was also seen to be constitutively associated with ICAM-1 both in nonstimulated (lane 1) and ICAM-1 stimulated cells (lanes 2-7).

LFA-1 associates with ICAM-1 following stimulation of T cells through ICAM-1. As shown in **Figure 2.4**, immunoblotting was performed as described previously and resulting blots were probed with anti-LFA-1 to assess whether LFA-1 is present in the ICAM-1 induced signaling complex. Since LFA-1 is present in large quantities in the pSMAC, we expected to either find that LFA-1 would not co-precipitate with ICAM-1 indicating that the ICAM-1 signaling complex is distinct from the SMACs associated

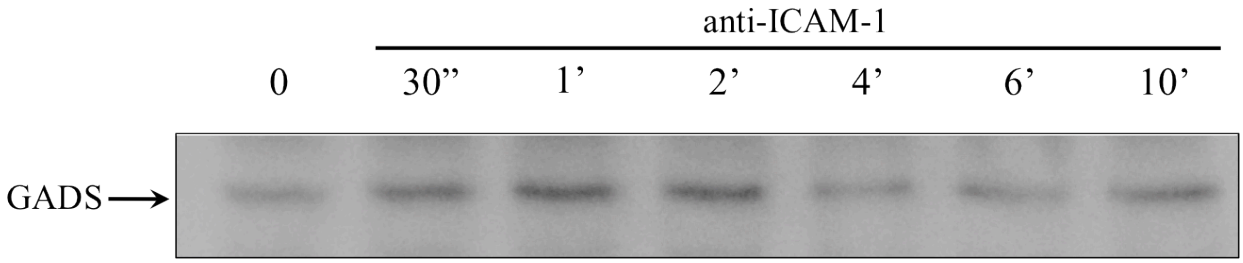
anti-ICAM-1
0
30”
1’
2’
4’
6’
10’
GADS

Figure 2.2. GADS is associated with ICAM-1
Lysates from tonsil T cells were prepared from cells stimulated through ICAM-1 and immunoprecipitated with anti-ICAM-1. The resulting immune complexes were resolved by SDS-PAGE, blotted onto PVDF and probed with anti-GADS. Lane 1, nonstimulated cells; Lanes 2-7, cells stimulated with anti-ICAM-1 for 30 seconds, 1, 2, 4, 6, and 10 minutes, respectively. The arrow indicates the apparent molecular weight that corresponds to the molecular weight of GADS, 37 kD. Representative of eight experiments.

Table 1

Signaling proteins found not to associate with ICAM-1 after stimulation through ICAM-1

Cbl
Vav
Gravin
SLP-76
Shc
Grb2
Sos

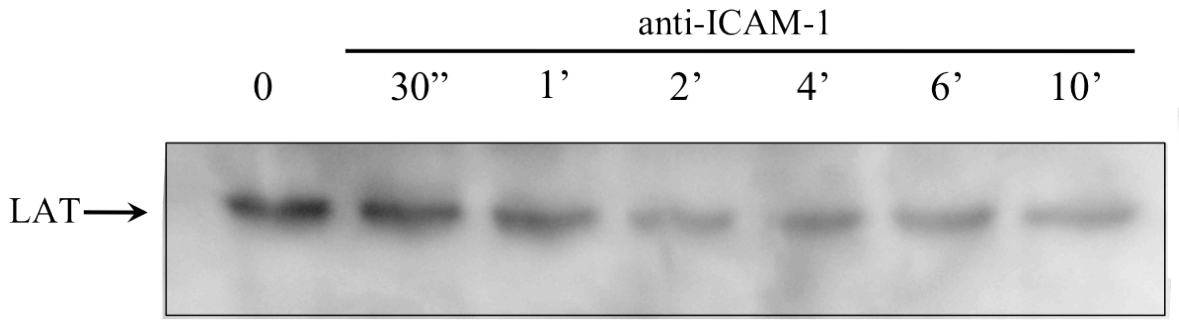
anti-ICAM-1
0
30”
1’
2’
4’
6’
10’
LAT

Figure 2.3. LAT is associated with ICAM-1
Lysates from tonsil T cells were prepared from cells stimulated through ICAM-1 and immunoprecipitated with anti-ICAM-1. The resulting immune complexes were resolved by SDS-PAGE, blotted onto PVDF and probed with anti-LAT. Lane 1, nonstimulated cells; Lanes 2-7, cells stimulated with anti-ICAM-1 for 30 seconds, 1, 2, 4, 6, and 10 minutes, respectively. The arrow indicates the apparent molecular weight that corresponds to the molecular weight of LAT, 36 kD. Representative of three experiments.

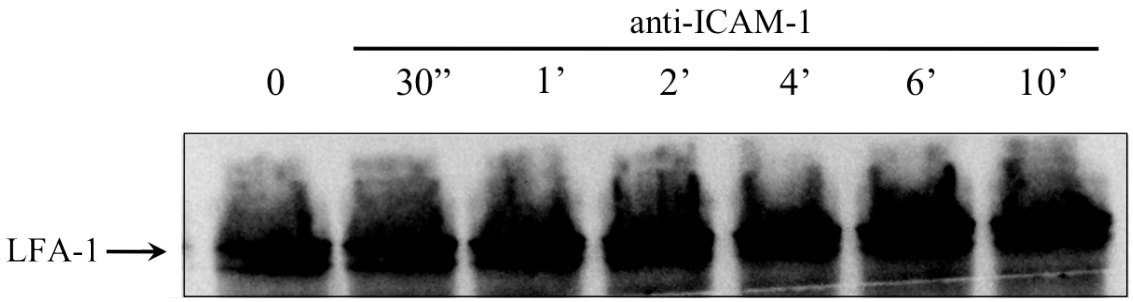
anti-ICAM-1
0
30”
1’
2’
4’
6’
10’
LFA-1

Figure 2.4. LFA-1 is associated with ICAM-1
Lysates from tonsil T cells were prepared from cells stimulated through ICAM-1 and immunoprecipitated with anti-ICAM-1. The resulting immune complexes were resolved by SDS-PAGE, blotted onto PVDF and probed with anti-LFA-1. Lane 1, nonstimulated cells; Lanes 2-7, cells stimulated with anti-ICAM-1 for 30 seconds, 1, 2, 4, 6, and 10 minutes, respectively. The arrow indicates the apparent molecular weight that corresponds to the molecular weight of LFA-1, 180 kD. Representative of three experiments.

with TCR signaling or present in large numbers within the ICAM-1 complex. We found the latter hypothesis to be true as we observed a thick band present at 180 kD indicating LFA-1 is associated with the complex.

CD45 associates with ICAM-1 following stimulation of T cells through ICAM-1. As shown in **Figure 2.5**, immunoblotting of total T cells was performed as described previously and the resulting blots were probed with a polyclonal antibody against CD45 recognizing the isoforms CD45RA and CD45RB. Since previous proteins involved in TCR-mediated signaling have been identified in the ICAM-1 induced complex, we expected CD45 to co-precipitate with ICAM-1. We observed that CD45 is constitutively associated with ICAM-1 throughout the duration of the initial signaling event (longer than 10 minutes after signaling through ICAM-1).

We also looked into the presence of individual isoforms of CD45. As shown in **Figure 2.6**, CD45RA, an isoform associated with naïve T cells, is shown to be associated with ICAM-1 at all timepoints. Interestingly, as shown in **Figure 2.7**, a different isoform, CD45RB, is notably absent immediately after stimulation through ICAM-1 (lanes 2-3), returning after 2 minutes (lane 4) and remaining associated with the complex thereafter (lane 5-7). While CD45 activates Lck by removing an inhibitory phosphate, CD45RB interferes with lipid raft localization thereby inferring with the activation state of Lck.

Fyn associates with ICAM-1 following stimulation of T cells through ICAM-1. Immunoblotting was performed as described previously and the resulting blots were probed with anti-Fyn. Since Dr. Chintana Chirathaworn identified Lck as being involved

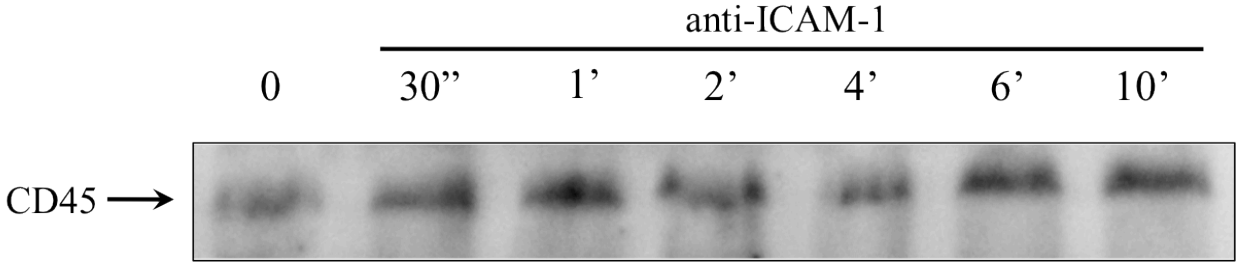
anti-ICAM-1
0
30”
1’
2’
4’
6’
10’
CD45

Figure 2.5. CD45 is associated with ICAM-1
Lysates from tonsil T cells were prepared from cells stimulated through ICAM-1 and immunoprecipitated with anti-ICAM-1. The resulting immune complexes were resolved by SDS-PAGE, blotted onto PVDF and probed with anti-CD45. Lane 1, nonstimulated cells; Lanes 2-7, cells stimulated with anti-ICAM-1 for 30 seconds, 1, 2, 4, 6, and 10 minutes, respectively. The arrow indicates the apparent molecular weight that corresponds to the molecular weight of CD45, 210 kD. Representative of three experiments.

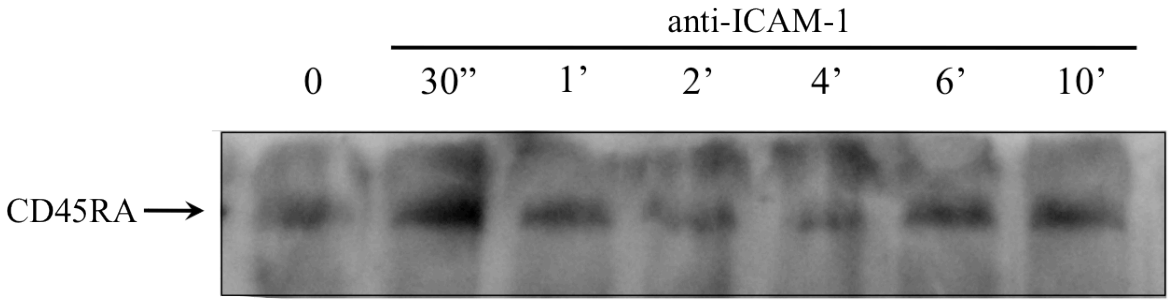
anti-ICAM-1
0
30”
1’
2’
4’
6’
10’
CD45RA

Figure 2.6. CD45RA is associated with ICAM-1
Lysates from tonsil T cells were prepared from cells stimulated through ICAM-1 and immunoprecipitated with anti-ICAM-1. The resulting immune complexes were resolved by SDS-PAGE, blotted onto PVDF and probed with anti-CD45RA. Lane 1, nonstimulated cells; Lanes 2-7, cells stimulated with anti-ICAM-1 for 30 seconds, 1, 2, 4, 6, and 10 minutes, respectively. The arrow indicates the apparent molecular weight that corresponds to the molecular weight of CD45RA, 205 kD. Representative of three experiments.

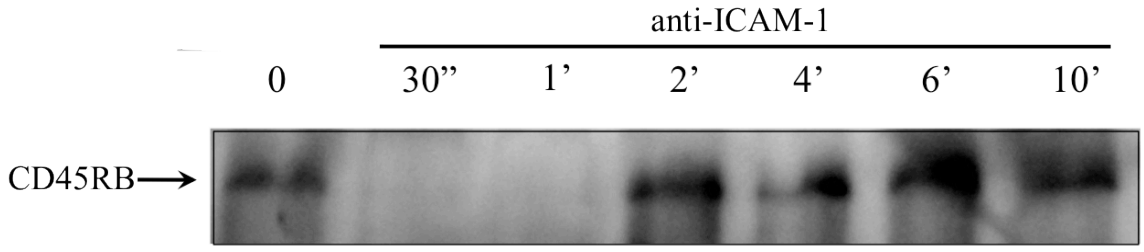
anti-ICAM-1
0
30”
1’
2’
4’
6’
10’
CD45RB

Figure 2.7. CD45RB is associated with ICAM-1
Lysates from tonsil T cells were prepared from cells stimulated through ICAM-1 and immunoprecipitated with anti-ICAM-1. The resulting immune complexes were resolved by SDS-PAGE, blotted onto PVDF and probed with anti-CD45RB. Lane 1, nonstimulated cells; Lanes 2-7, cells stimulated with anti-ICAM-1 for 30 seconds, 1, 2, 4, 6, and 10 minutes, respectively. The arrow indicates the apparent molecular weight that corresponds to the molecular weight of CD45RB, 220 kD. Representative of three experiments.

in the signaling complex, we hypothesized that Fyn would also be associated since both Src family kinases are involved in TCR-mediated signaling. As shown in **Figure 2.8**, Fyn associates with the complex 2 minutes after initial stimulation and leaves the complex by 4 minutes. The kinetics that Fyn exhibits is identical to those observed for Lck. Interestingly the band that corresponds to the apparent molecular weight of Fyn is consistently dim which may indicate a weak association with the signaling complex although Fyn is traditionally pale in this type of western blot.

ICAM-1 stimulation clustered lipid rafts to the site of engagement. Antibody-coated beads were incubated with fixed and biotinylated-CtxB stained Jurkat cells for 5 minutes and counterstained with streptavidin-Cy3 to visualize lipid rafts. The non-toxic β subunit of Cholera toxin binds to the ganglioside GM1 present in rafts and allows for imaging of the location of lipid rafts on the surface of cells. As shown in **Figure 2.9**, antibody stimulation using anti-ICAM-1 (*C* and *D*), anti-ICAM-1+anti-CD3 (*E* and *F*) or anti-CD28+anti-CD3 (*G* and *H*) coated beads resulted in polarization of lipid rafts toward the antibody-coated bead.

The percentage of T cell:bead conjugates with lipid raft polarization was quantified for both ICAM-1 alone (**Figure 2.10**) and for anti-CD3+anti-ICAM-1 and anti-CD3+anti-CD28 (**Figure 2.11**) as compared to the isotype control.

Previous studies and experiments described in this chapter have identified several intracellular proteins involved in receptor-mediated lymphocyte activation in response to stimulation through ICAM-1. The complex identified thus far includes Src family kinases

Lck and Fyn, CD3ζ, TCRβ, MAPK, cdc2, LFA-1, the CD45 isoforms CD45RA and CD45RB, and the adaptor proteins Gads and LAT.

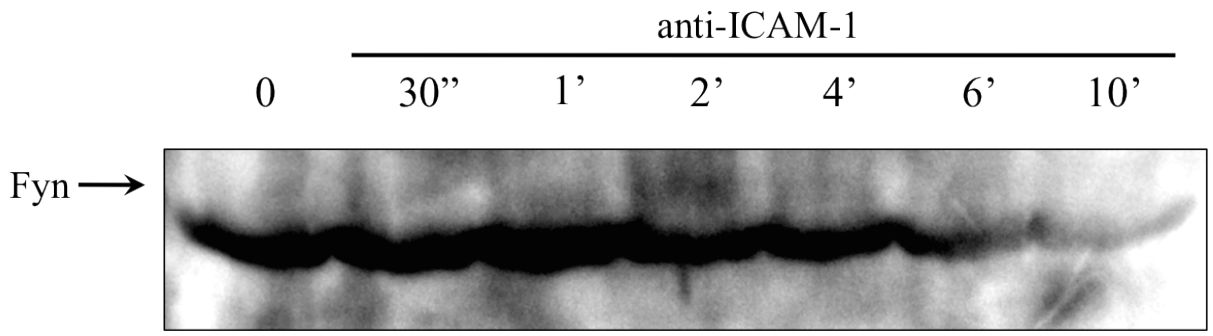
anti-ICAM-1
0
30”
1’
2’
4’
6’
10’
Fyn

Figure 2.8. FYN is associated with ICAM-1
Lysates from tonsil T cells were prepared from cells stimulated through ICAM-1 and immunoprecipitated with anti-ICAM-1. The resulting immune complexes were resolved by SDS-PAGE, blotted onto PVDF and probed with anti-FYN. Lane 1, nonstimulated cells; Lanes 2-7, cells stimulated with anti-ICAM-1 for 30 seconds, 1, 2, 4, 6, and 10 minutes, respectively. The arrow indicates the apparent molecular weight that corresponds to the molecular weight of FYN, 59 kD. Representative of seven experiments.

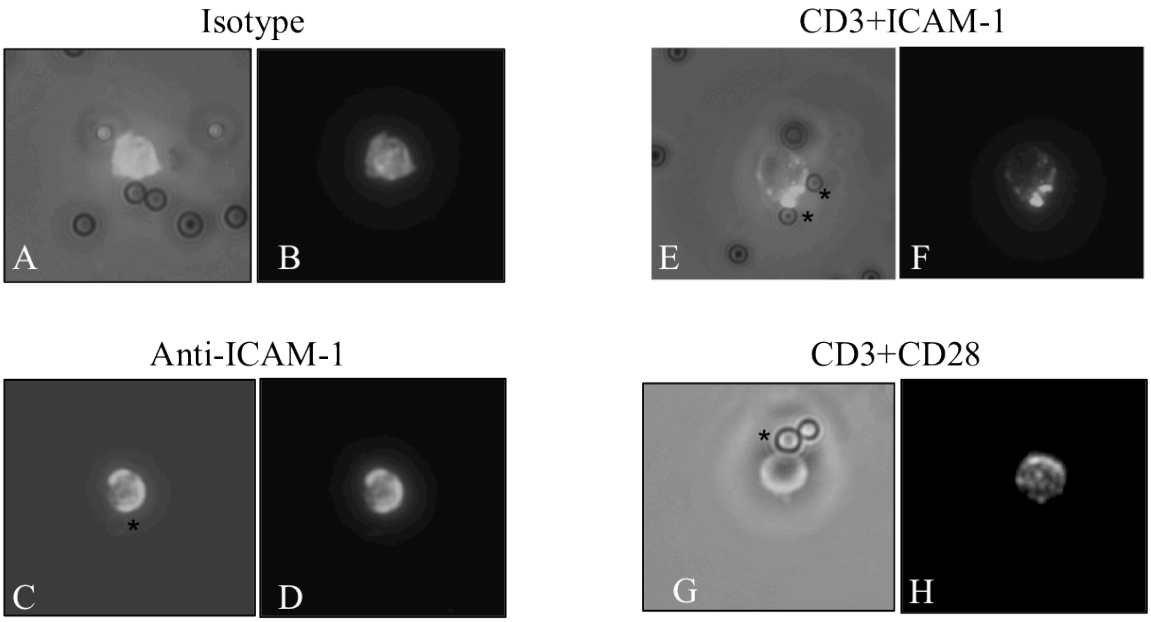
Isotype
A
B
CD3+ICAM-1
E
F
Anti-ICAM-1
C
D
CD3+CD28
G
H

Figure 2.9. Antibody stimulation clusters lipid rafts to the site of engagement

Jurkat T cells were stained with biotinylated Ctx-B, incubated with isotype (*A* and *B*), anti-ICAM-1 (*C* and *D*), anti-CD3+anti-ICAM-1 (*E* and *F*) or anti-CD3+anti-CD28 (*G* and *H*) coated beads for 30 minutes, fixed and counterstained with streptavidin-Cy3. * indicates location of the antibody-coated bead. Representative of four experiments.

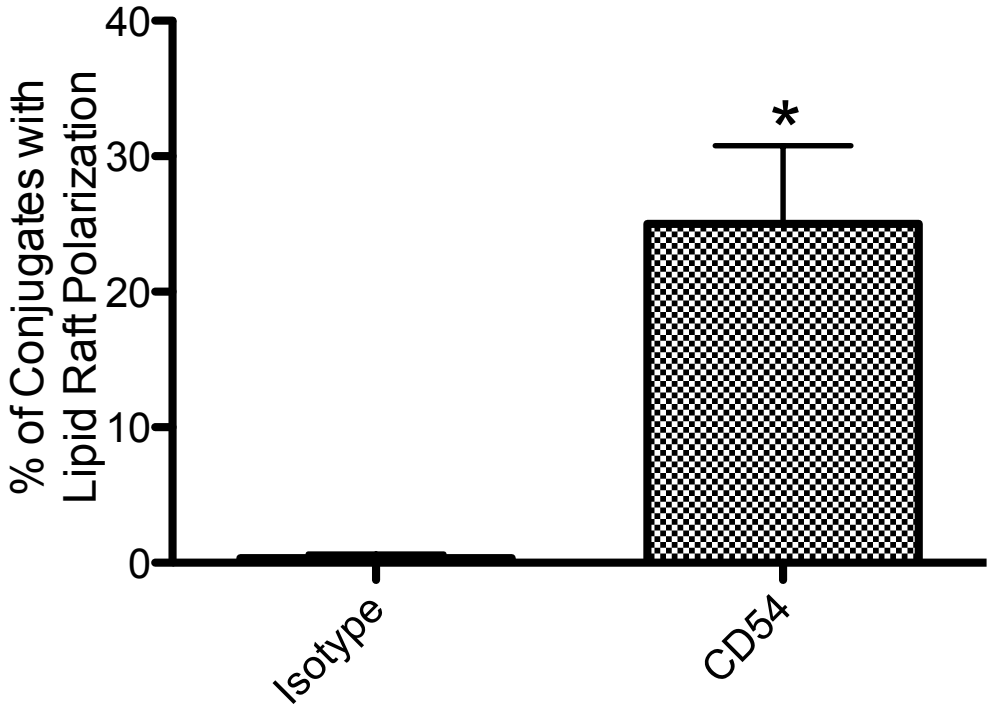
% of Conjugates with Lipid Raft Polarization
40
30
20
10
0
*
Isotype
CD54

Figure 2.10. ICAM-1 stimulation clusters lipid rafts to the site of engagement

Jurkat T cells were stained with biotinylated Ctx-B, incubated with isotype or anti-ICAM-1 (CD54) coated beads for 30 minutes, fixed and counterstained with streptavidin-Cy3. Lipid raft polarization was quantified using 20 random representative cell:bead interactions. Representative of four experiments. * = $p<0.05$

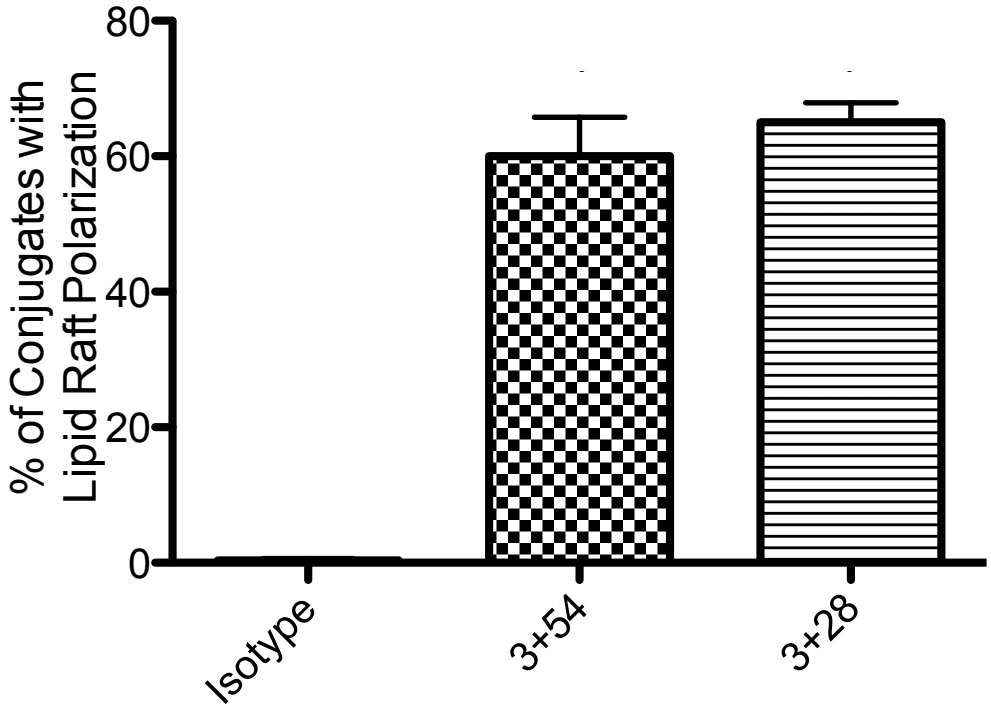
% of Conjugates with Lipid Raft Polarization
80
60
40
20
0
Isotype
3+54
3+28

Figure 2.11. CD3+ICAM-1 stimulation induces lipid raft polarization to a similar level as stimulation through CD3+CD28
Jurkat T cells were stained with biotinylated Ctx-B, incubated with isotype, anti-CD3+anti-ICAM-1, anti-CD3+anti-CD28 coated beads for 30 minutes, fixed and counterstained with streptavidin-Cy3. Lipid raft polarization was quantified using 20 random representative cell:bead interactions. Representative of four experiments. * = $p<0.05$

Discussion

As detailed in Chapter 1, ICAM-1 signaling has been associated with rearrangement of the actin cytoskeleton, temporary cell cycle arrest and intracellular calcium release following activation. The pathways activated by ICAM-1 signaling remain poorly understood and of great interest in our lab. Dr. Chintana Chirathaworn previously demonstrated that ICAM-1 stimulation leads to transient phosphorylation and inactivation of cdc2 kinase, as well as the association of Mitogen Activated Protein (MAP) kinases ERK1 and ERK2, ZAP-70 and the Src family kinase, Lck. Chintana observed that the TCR signaling intermediate ZAP-70 is phosphorylated upon ICAM-1 engagement. Additional work has also shown that Lck is activated shortly after ICAM-1 triggering, with maximal phosphorylation observed by 2 minutes. ERK1 and ERK2 also were shown to become activated following ICAM-1 stimulation.

In addition to the experiments showing kinase activation by ICAM-1 stimulation, Chintana also observed involvement of the TCR, CD3ζ chain, MAP kinases (**Figure 2.1**). Additional work detailed in this chapter has further expanded our knowledge of the complex to include CD45RA, CD45RB, LFA-1, Fyn and the adaptor proteins LAT and Gads (**Figure 2.12**).

Previous work done in the lab to identify an adaptor protein capable of mediating the ICAM-1 induced signaling complex was largely unsuccessful. Adaptor proteins are commonly found in signaling complexes and directly couple signaling proteins to each other. Adaptor proteins usually lack enzymatic activity, but contain SH2 and/or SH3 domains that allow for protein-protein interaction. SH2 domains recognize specific

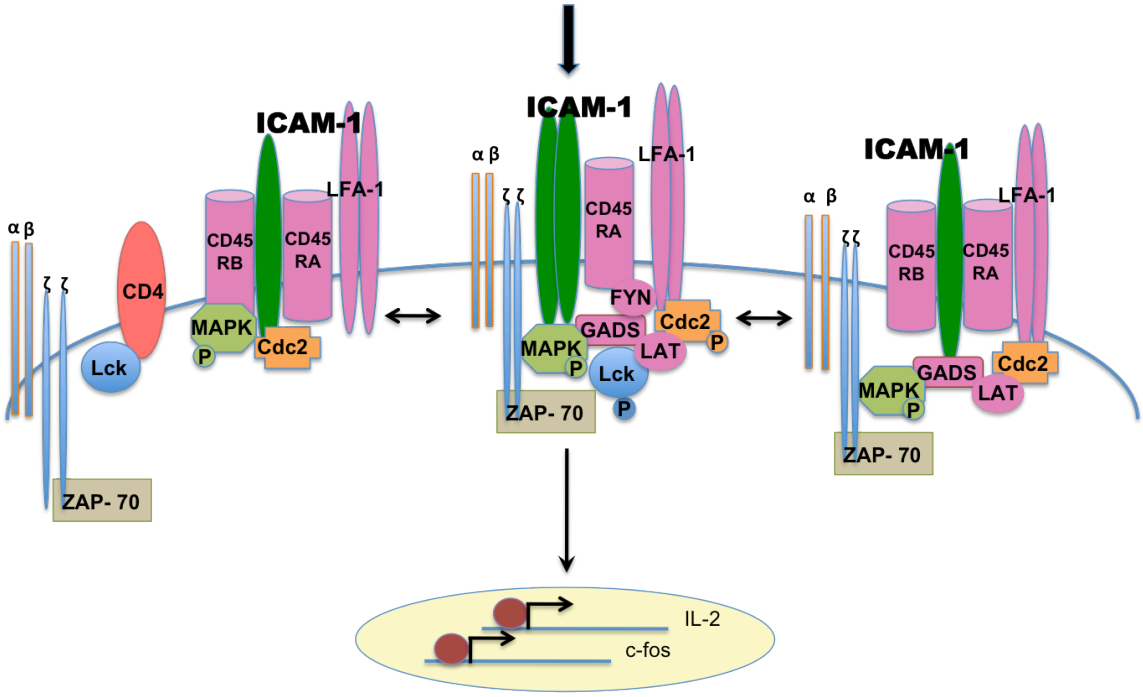
ICAM-1
ICAM-1
ICAM-1
LFA-1
LFA-1
LFA-1
α β
α β
α β
ζ ζ
ζ ζ
ζζ
CD4
CD45 RB
CD45 RA
CD45 RB
CD45 RA
CD45 RA
CD45 RB
CD45 RA
MAPK
P
Cdc2
Lck
FYN
GADS
Cdc2
P
MAPK
P
LAT
Lck
P
GADS
Cdc2
MAPK
P
LAT
ZAP- 70
ZAP- 70
ZAP- 70
IL-2
c-fos

Figure 2.12. The ICAM-1 Signaling Complex
Previous studies identified the association and activation of the kinases Lck, ERK1, ERK2 and cdc2 upon antibody stimulation through ICAM-1. In addition to the associated kinases, LFA-1 and CD45RA are constitutively associated with ICAM-1. FYN is associated with ICAM-1 only after 4 minutes and thereafter leaves the complex. LAT associates with ICAM-1 upon stimulation and remains associated throughout the duration of the experiment. Proteins colored in pink represent those identified through experiments presented in this thesis.

tyrosine phosphorylated proteins and are highly conserved. Like SH2 domains, SH3 domains are highly conserved, present in a variety of signaling molecules and recognize proline-rich sequences.

Common adaptor proteins involved in T cell signaling such as Shc, Grb2, SLP-76, Cbl and Sos were not observed in immunoprecipitation experiments upon stimulation through ICAM-1 (**Table 1**). Dr. Jake Kohlmeier hypothesized that a lack of adaptor protein may be attributable to the possibility that proteins involved in the ICAM-1 signaling complex are not associated through direct protein-protein interactions, but brought into close proximity by lipid rafts. While lipid rafts play a major role in bringing together signaling molecules, it appears that the ICAM-1 signaling complex is at least in part mediated by protein-protein interactions involving the adaptor protein Gads.

Gads has been shown to interact specifically with SLP-76 via the SH3 domain and LAT via the SH2 domain. While SLP-76 is a substrate of ZAP-70 and is actively involved in TCR-mediated signaling, it was not present in the ICAM-1 complex. The absence of SLP-76 as well as the absence of many other traditional proteins involved in TCR signaling (**Table 1**) coupled with the presence of active kinases may indicate that ICAM-1 signaling is mediated by a novel complex. While this tends to be the favored hypothesis, it also is possible that ICAM-1 signaling may drag CD3-associated signaling intermediates into the rather large complex unintentionally. This seems unlikely though given the specific activation of kinases and their transient association with the complex.

The presence of LFA-1 in the complex indicates that supramolecular activation clusters, specifically the pSMAC, may be involved in ICAM-1 mediated signaling. LFA-1 would be expected to associate given the major role the molecule plays in mediating

cell adhesion during signaling. The presence of LFA-1 would be necessary to allow for both a strong and prolonged interaction between two communicating cells.

While LFA-1 was shown to co-precipitate with anti-ICAM-1 (**Figure 2.4**), the possibility exists that its presence in the complex is due to protein-protein interactions on the surface and not because of a direct association with the complex. Testing of the ability of LFA-1 and ICAM-1 to interact with each other on the surface of the same cell is of some interest in our lab and future work on this may shed further light on LFA-1 presence within the complex.

Because LFA-1 co-precipitated with ICAM-1 as well as other major cell signaling proteins like Lck, we expected CD45 to also be present in the complex. Since several isoforms of CD45 exist, we looked into the possibility that different isoforms may have differing roles within complex formation. Blots were probed with CD45RA, the isoform associated with naïve T cell populations, and CD45RB, a lesser known isoform the presence of which negatively regulates lipid raft formation (60). CD45RA was seen to be associated with ICAM-1 at all timepoints as seen in Figure 5, however CD45RB is only associated with ICAM-1 prior to stimulation and after 2 minutes (**Figure 2.7**). The RB isoform is notably absent immediately after stimulation during the crucial initial signaling events. While CD45 is known to activate Lck by removing an inhibitory phosphate, CD45RB has been shown to interfere with lipid raft localization and thus the activation state of Lck. The timing of CD45RB transient absence from the complex is interesting especially when coupled with the timing of Lck and Fyn activation. The timing suggests that CD45RB moves out of the complex after initial signaling to allow for the activation of Lck seen at 2 minutes. It also is intriguing that the disappearance of active Lck from

the complex coincides with the reappearance of CD45RB. Future studies into the direct association of Lck and CD45RB in the context of ICAM-1 signaling should be examined.

The polarization of lipid rafts is thought to be requisite for successful T cell activation as demonstrated by the observation that dispersal of lipid rafts inhibits full activation (44). In **Figure 2.9**, stimulation through ICAM-1 alone caused lipid rafts to coalesce near the antibody-coated bead suggesting that signaling through ICAM-1 may promote synapse formation by directing lipid rafts and their associated signaling molecules toward the site of cell contact. As shown in **Figure 2.10**, the increase in the percentage of cell:bead conjugates with lipid raft polarization upon stimulation with anti-ICAM-1 was statistically significant when compared to the isotype control. This indicates that the lipid raft polarization seen is a direct consequence of signaling through ICAM-1 and not simply a non-specific antibody interaction.

As expected, addition of anti-CD3 to ICAM-1 or CD28 coated beads dramatically increased the percentage of conjugates showing raft polarization (**Figure 2.11**). It should also be noted that while ICAM-1 alone can induce polarization of lipid rafts, the addition of anti-CD3 increases the percentage to that seen with anti-CD3 and the traditional costimulatory molecule, CD28. While the lab has published and extensively studied the role of ICAM-1 as a costimulatory molecule, the ability of ICAM-1 to induce lipid raft formation to the same extent as CD28 further advances the importance ICAM-1 has in signaling.

While the hallmarks of a traditional signaling event have been well characterized regarding the signaling complex associated with ICAM-1, the evolutionary reasoning for the complex dynamics remains elusive. Our working hypothesis centers around the idea

that ICAM-1 functions to nucleate a complex termed “signal zero” by our lab. As a specific T cell searches for its cognate antigen, the ICAM-1 signaling complex keeps important signaling molecule ready to fire immediately upon binding of the TCR to antigen presented on MHC. If the T cell samples non-cognate antigen presented on MHC, the once ready-to-fire complex disassociates and the TCR moves on to sample other peptide:MHC complexes on the cell and eventually detaches and moves on to the next APC. If the T cell binds cognate antigen, the complex can immediately coalesce lipid rafts containing the necessary signaling molecules to induce full activation and allows for an immediate response to the foreign antigen. While the data supports this model, we have yet to determine a definitive way to test the “signal zero” hypothesis. Identification of cdc25 within the complex, the phosphatase that inactivates cdc2, as well as functional studies looking at cdc2 activity upon CD3 stimulation are planned. These and other future studies within the lab will no doubt focus on ways to determine the evolutionary significance of the ICAM-1 induced signaling complex.

Chapter 3:

Evaluation of a short dose of therapeutic peptides in treating murine type I diabetes in the non-obese diabetic model

Introduction

Type I diabetes mellitus, also known as juvenile diabetes or insulin-dependent diabetes mellitus, is a chronic autoimmune disorder characterized by the destruction of pancreatic β-cells in the islets of Langerhans. The attack on pancreatic β-cells is driven by T-cell induced autoimmunity. Self-reactive T cells infiltrate the pancreatic islets where they induce β-cell destruction (61). This unchecked attack on pancreatic β-cells leads to the inability of the pancreas to adequately control blood glucose levels and the development of overt insulitis.

The non-obese diabetic (NOD) mouse is an experimental animal model for Type I diabetes. The strain is polygenic with specific polymorphisms in the gene for interleukin 2 and the mitochondrially encoded tRNA arginine as well as a deletion of the hemolytic complement gene. The strain was originally identified through spontaneous development of polyuria and glysuria by a female cataract Shionogi (CTS) mouse (62). The subsequent development of the NOD-strain allowed for an approach to not only study the pathogenesis of disease, but also opened the door for potential therapeutic approaches targeting Type I diabetes to be examined.

As with any T-cell mediated autoimmune disease, the problem with development of an effective therapy is specificity. Current therapeutic approaches for autoimmunity focus on a global knockdown of either the entire adaptive immune response through immunosuppressants or a knockdown of T cells (including both self-reactive and non self-reactive) through targeting specific T cell signaling pathways.

The method of choice for specific T cell targeting is through the use of monoclonal antibody therapy. While some monoclonal antibodies have proven effective in treatment of various diseases, treatment can produce harmful side effects including urticaria, leucopenia and potential allosensitization to the antibody itself (64-66). Developing a specific treatment for Type I diabetes has proven difficult. Teplizumab, a promising humanized anti-CD3 monoclonal, showed preclinical promise in protecting remaining β-cells and mediating active disease in mouse models and in *in vitro* studies (63). However, recently the therapy had disappointing results in Phase III clinical trials showing no benefit to treatment in patients with Type I diabetes.

The best approach for therapy would be one where self-tolerance could be restored by induction of self-reactive T cell anergy or death. This approach would then leave the self-tolerant cells intact and able to respond to infection and eliminate only those involved in Type I diabetes. Ideally this therapy would also be as specific as a monoclonal antibody, but without the harmful side effects.

The use of short peptides in treatment of autoimmune disorders has shown extensive promise in our lab. Dr. Scott Tibbetts developed short peptides derived from the ICAM-1 and LFA-1 contact domains that have shown to be effective in treating autoimmune arthritis in a collagen-induced arthritis (CIA) model (**Table 2**). The safety of the peptides also was tested and peptides were found to not alter cell viability or number even when used at a 2-fold higher concentration.

The proposed mechanism is based on blocking both adhesion and costimulation through LFA-1/ICAM-1 blockade. As detailed in Chapter 1, antigen-specific TCR present on a T-cell interacts with antigen being presented by MHC on an APC. This first

signal (termed signal 1) provides specificity for the T cell response by initiating T cell activation only if the antigen is cognate. In the case of autoimmune disease, the self-reactive T cells activate when self-antigen is encountered. For full activation to occur, a second costimulatory signal (termed signal 2) must be present. As discussed in Chapter 1, both proteins targeted by the peptides, ICAM-1 and LFA-1 are capable of acting as costimulatory molecules. If signal 1 is delivered, but signal 2 is blocked, the T cell either undergo apoptosis or are rendered anergic and unable to function.

The proposed induction of tolerance by the peptide treatment is based on allowing the self-reactive T cell to encounter antigen (in the case of T1D, β-cell specific antigens) thus allowing for signal 1, but blocking LFA-1/ICAM-1 second signals rendering the cells dead or anergic.

Dr. Abby Dotson has successfully shown a delay in T1D disease progression when treating NOD mice with 14 injections of the peptides administered over the course of 4 weeks. A delay in the increase of blood glucose levels as well as an elimination of T cell reactivity were seen when animals were treated with 50 μg of each peptide (100 μg total). While Abby had success using this course of treatment, we wanted to see if using a shortened dosing regimen would be as successful. The following short dose experiment was done in collaboration with Dr. Abby Dotson

In both the CIA and T1D experiments, long courses of treatment with peptides were used. Scott treated animals using alternate day injections throughout the entire 8-week experiments while Abby treated with a 14 injections regimen. Previous work done by Isobe et al showed survival of cardiac allografts using a 6-day course of monoclonal antibodies to both ICAM-1 and LFA-1 (67). Since we have had success with treatment of

T1D using the peptide therapy, we tested the effectiveness of a short dose regimen on mediating T1D disease progression. The work presented in this chapter shows the effectiveness of treating NOD-mice with a short doge regimen of LFA-1/ICAM-1 derived peptides.

Table 2

Peptides derived from LFA-1 and ICAM-1

Peptide	Protein Sequence	Peptide Sequence	Source	Region
cLAB-L	ITDGEATDSGNIDAAKDII	penITDGEATDSGC	LFA-1α	237-246
cIE-L	DQPKLLGIETPLPKKELLL	penDQPKLLGIETC	ICAM-1	26-35

Table 2. Peptides derived from LFA-1 and ICAM-1.
The first letter of the peptide name denotes the origin of the peptide. For example, ‘LAB-L’ is derived from the LFA-1α subunit, while ‘IE-L’ is derived from ICAM-1. The prefix ‘c’ indicates the peptides were cyclized. ‘Pen’ stands for penicillamine, a residue that facilitates in cyclization of the peptide.

Materials and Methods

Mice. Female NOD/ShiLtJ mice (Jackson Laboratories) were obtained at 8 weeks of age and were housed individually in barrier cages. Animal experiments were performed with approval from the University of Kansas Animal Care and Use Committee.

Peptides. Peptides were prepared and cyclized shown in Chapter 2. Cyclized peptides were purchased from American Peptide Company. Lyophilized peptides were stored desiccated at -20^{o}C until use. Immediately prior to use, peptides were resuspended in normal saline at 1μg/μl. For i.v. injections, 50 μl c-IE-L and 50 μl cLAB-L were mixed immediately prior to injection.

Peptide therapy and diabetes monitoring. Fasting blood glucose levels (BGL) were monitored weekly prior to treatment using the OneTouch Ultra 2 glucometer and OneTouch Ultra Blue test strips (LifeScan). Fasting levels were determined by removing food 2 h before each BGL reading. Saline and therapeutic peptides were injected at 48 h intervals beginning at 12 weeks of age until 14 weeks of age. Peptide treated mice received a total of 7 injections over the course of 2 weeks. Mice were considered diabetic after two consecutive BGL readings >250 mg/dL. When mice were sacrificed due to severity of disease, a BGL of 600 mg/dL was used thereafter in the calculations for those mice.

Pancreas imaging. Pancreata were harvested from treated or control mice and paraffin-embedded for sectioning. 10 μm planar slices were cut, placed on slides and stained with hematoxylin and eosin. Pancreas sections were photographed using a Zeiss Axioscope photomicroscope at 40X magnification.

Scoring of islets and the stages of islet destruction. Hematoxylin and eosin stained images of pancreatic islets were observed and analyzed for insulitis. All islets identified were photographed and the resulting images were scored for islet infiltration as described previously (69). Briefly, Pre-insulitis is characterized by no infiltration of leukocytes into the islet. Peri-insulitis is characterized by margination of leukocytes along the outside of the islet and is indicative of the early stages of infiltration. Intra-insular insulitis is characterized by a later stage of infiltration where the majority of the islet has been infiltrated with leukocytes. Complete islet destruction is characterized by the complete infiltration of the islet by leukocytes (**Figure 3.1**).

Adoptive transfer. Spleens were harvested from control or peptide treated NOD mice at 22.5 weeks of age, minced and repeatedly pressed with a 1cc syringe plunger through a sterile 70 μm nylon mesh cell strainer. Erythrocytes were cleared by a five-minute incubation of the cell suspension in ACK lysis buffer (0.15M NH_4Cl, 10mM $KHCO_3$, 0.1mM Na_2EDTA, pH 7.2) at 37^oC. The resulting cell mixture was purified using a mouse total T cell magnetic separation kit and column (StemSep). After purification, 5 x 10^6 total T cells were injected into NOD-SCID mice via tail vein injections. Blood glucose levels were monitored weekly for 6 weeks post adoptive transfer (**Figure 3.2**).

Statistical analysis. Statistical analysis was performed using GraphPad Prism (GraphPad Software).

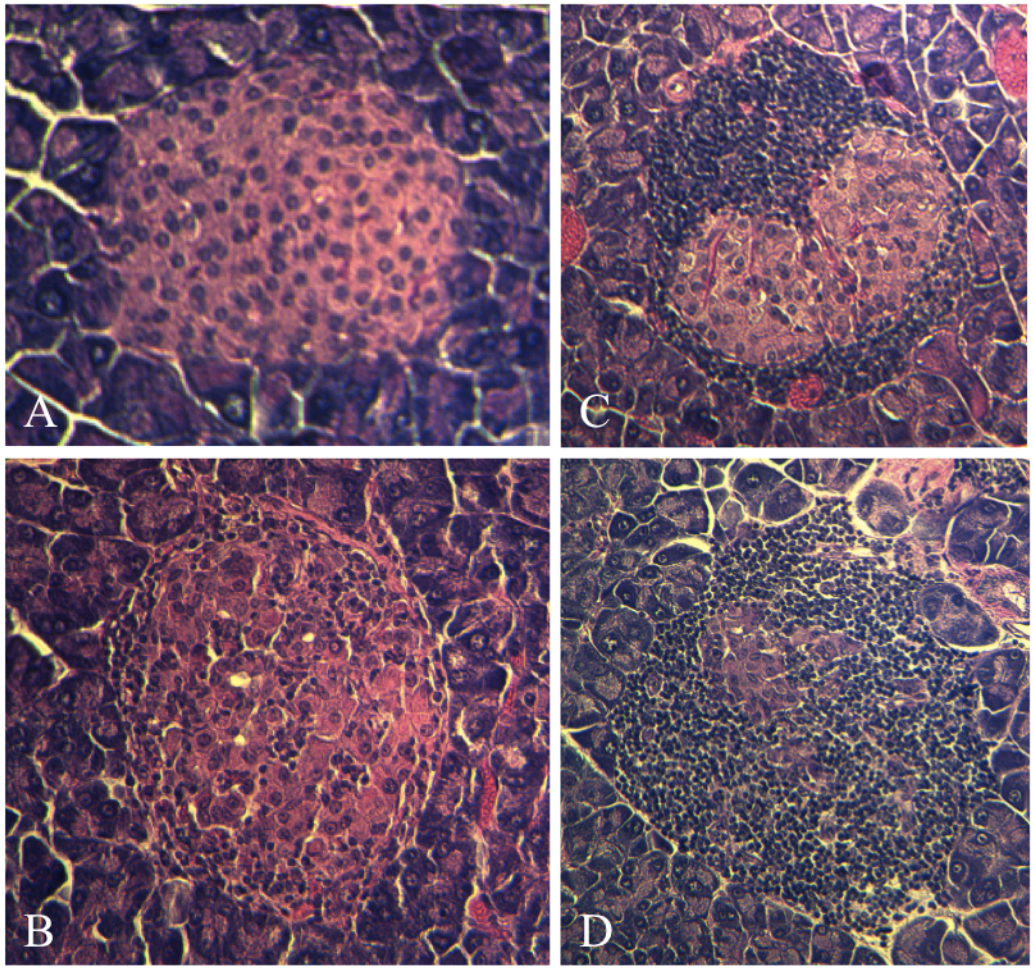
A
C
B
D

Figure 3.1. Representative images of the stages of islet destruction
Pre-insulitis (*A*) is characterized by no infiltration of leukocytes into the islet. Peri-insulitis (*B*) is characterized by margination of leukocytes along the outside of the islet and is indicative of the early stages of infiltration. Intra-insular insulitis (*C*) is characterized by a later stage of infiltration where the majority of the islet has been infiltrated with leukocytes. Complete islet destruction (*D*) is characterized by the complete infiltration of the islet by leukocytes.

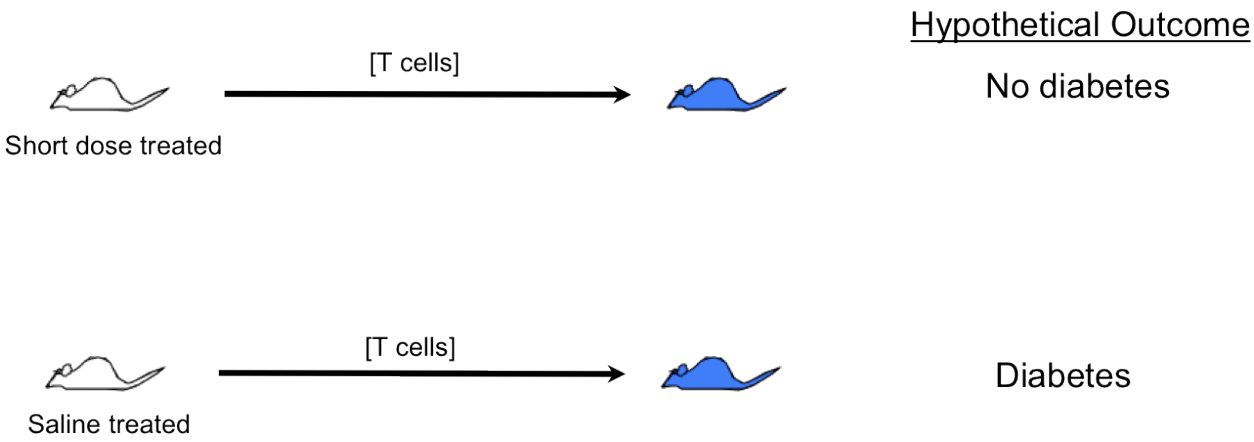
Hypothetical Outcome
[T cells]
No diabetes
Short dose treated
[T cells]
Diabetes
Saline treated

Figure 3.2. Schematic of the adoptive transfer experiment
Splenic T cells were harvested from both saline control and short dose treated mice and transferred to NOD-SCID mice via tail vein injection. T cells taken from the saline control mice were split into two groups and either directly injected via tail vein or incubated *in vitro* with 250 μM each of cLAB-L and cIE-L prior to injection.

Results

Short dose regimen of peptide caused a delay in the incidence of diabetes. Mice were acquired at 8 weeks of age with an average BGL of 96 mg/dL. Glucose levels were monitored weekly until mice were 12 weeks of age and mice were randomly assigned to either saline or peptide treated groups (n=5 mice per group). The average BGL of each group was roughly 110 mg/dL. The increase in blood glucose levels at this age correlates with the observation that insulitis begins to occur as early as 3-4 weeks of age and the pancreatic insulin content begins to decrease at 12 weeks of age (68). We determined that the mice were in the initial stages of diabetes onset.

Once the groups were established, mice were injected with either normal saline or a combination of cIE-L and cLAB-L for a total peptide dose of 100 μg per injection at 48 hour intervals. Blood glucose levels were measured at each injection and monitored weekly for an additional 12 weeks after the course of treatment was initiated. As shown in **Figure 3.3**, mice receiving the saline injections exhibited an elevated BGL starting as soon as treatment was stopped and became overtly diabetic (BGL >250 mg/dL) within 3 weeks after cessation of therapy (dashed line). In contrast to the saline control mice, the peptide treated mice never developed an increase in the blood glucose levels even past 80 days post therapy initiation (solid line).

Islets of mice receiving peptide treatment show a reduction in leukocyte infiltration. Islets from mice were stained with hemotoxylin and eosin, quantified and classified according to the level of infiltration described in the *Materials and Methods*. Examples of each

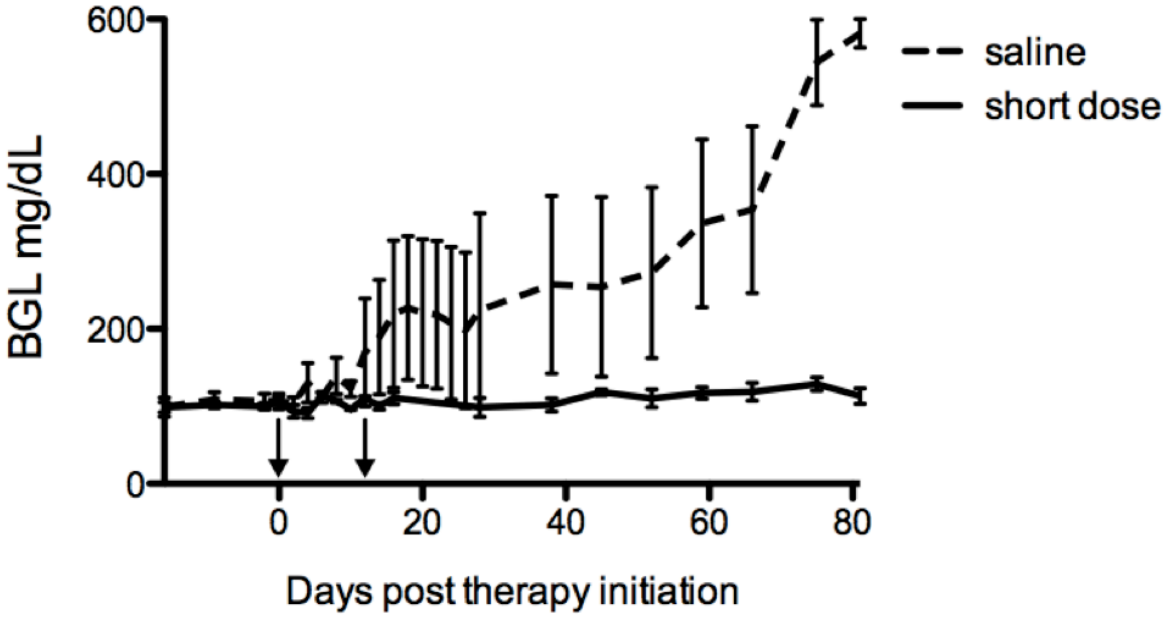
600
400
200
0
BGL mg/dL
0
20
40
60
80
Days post therapy initiation
saline
short dose

Figure 3.3. The onset of diabetes is delayed in mice treated with a short dose of peptide therapy
NOD mice received injections on alternate days via tail vein of either normal saline (dashed line; 14 injections) or a combination of 50 µg cIE-L and 50 µg cLAB-L (solid line; 7 injections) . Fasting blood glucose levels (BGL) were measured at time of injection and monitored weekly after administration of treatment. Average BGL is shown for each group (n=5 mice per group). Arrows indicate the start and completion of injections. Figure completed in collaboration with Dr. Abby Dotson.

stage of infiltration can be seen in Figure 14. The degree of infiltration was scored and the quantification can be seen in **Figure 3.4**. 22 islets from the saline injection group and 32 islets from the peptide treated group were imaged and assessed for the degree of insulitis. In the saline treated mice, over 60% of the islets were completely destroyed as characterized by complete infiltration of the islet by leukocytes. A small percentage of the islets were shown to be in the early-middle and middle-late stages of infiltration, peri-insulitis and intra-insular insulitis, respectively. Only 22% of the islets were scored as pre-insulitis, indicating no infiltration had occurred and the islets were healthy and intact.

In contrast, the mice treated with the short dose peptide regimen had the majority of the islets fall into the pre-insulitis category indicating the vast majority of islets in the treated animals were healthy. Only 21% of the short dose treated islets fell into the later three stages of peri-insulitis, intra-insular insulitis or complete islet destruction.

Adoptively transferred T cells harvested from short dose treated mice do not induce diabetes in NOD-SCID mice. Total T cells were harvested from the spleens of either saline or short dose treated mice and injected into NOD-SCID mice. NOD-SCID mice lack endogenous T and B cells and therefore do not develop type 1 diabetes as seen in the NOD model. Due to the inability of the NOD-SCID model to develop diabetes without exogenous T cell transfer, their blood glucose levels remain constant and never increase throughout their lifespan (70). As shown in **Figure 3.5**, NOD-SCID mice that received adoptively transferred T cells from saline control NOD mice developed overt diabetes within 3 weeks. In direct contrast, the NOD-SCID mice receiving cells from the short

dose treated mice did not have an increase in blood glucose level even when monitored past 40 days post adoptive transfer.

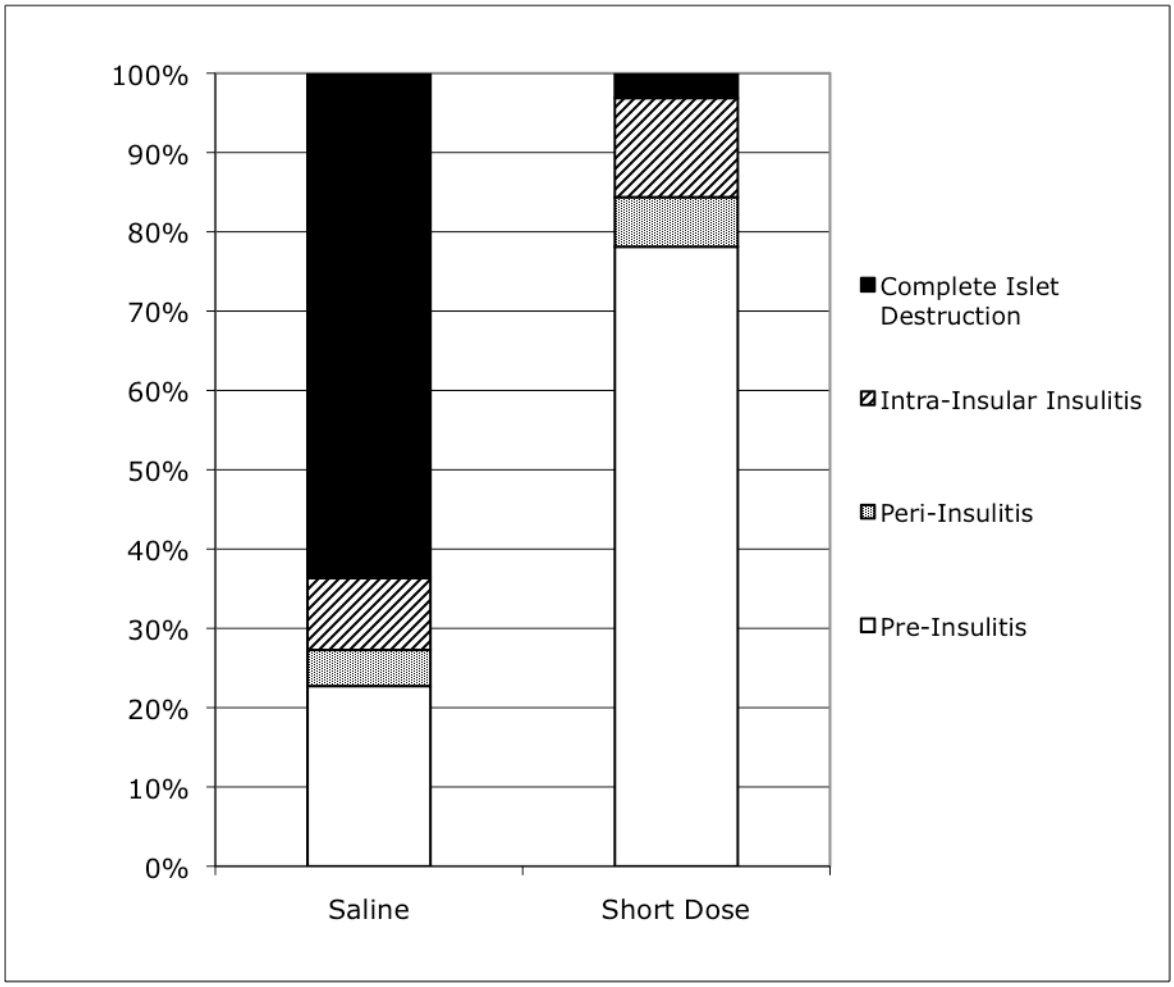
100%
90%
80%
70%
60%
50%
40%
30%
20%
10%
0%
Saline
Short Dose
Complete Islet Destruction
Intra-Insular Insulitis
Peri-Insulitis
Pre-Insulitis

Figure 3.4. Islets of mice treated with peptide therapy show a reduction in leukocyte infiltration
Islets from saline and peptide treated mice were stained with hematoxylin and eosin, quantified and classified according to the level of infiltration. n=22 and 32 islets per group from 4 saline control mice or 5 peptide treated mice.

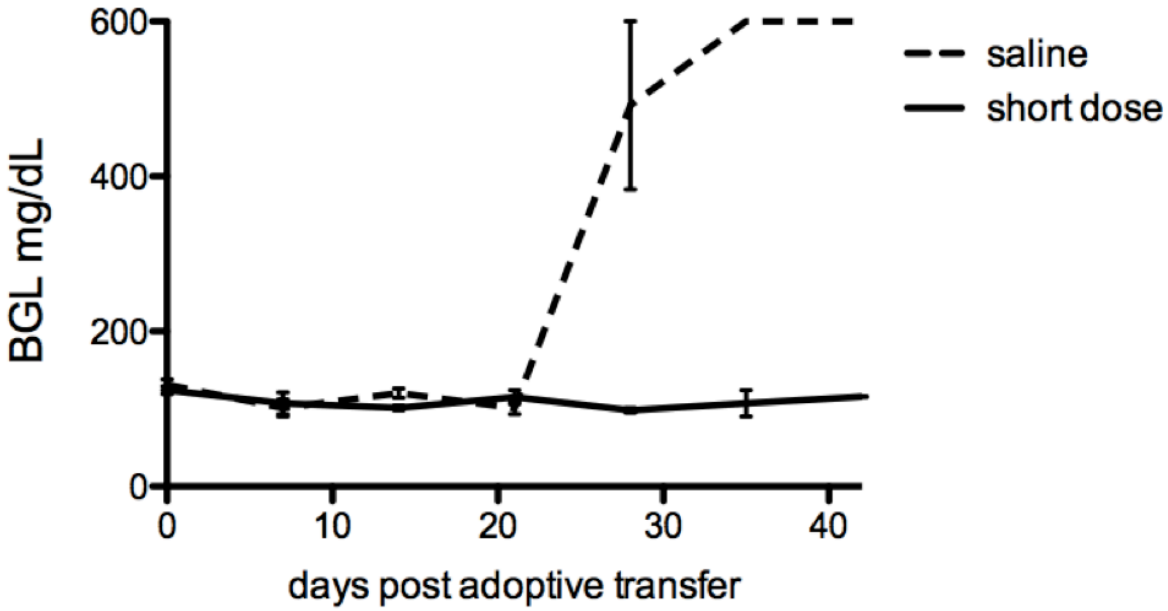
600
400
200
0
BGL mg/dL
0
10
20
30
40
days post adoptive transfer
saline
short dose

Figure 3.5. Adoptively transferred T cells harvested from short dose treated mice do not induce diabetes in NOD-SCID mice
Total T cells harvested from the spleens of either saline control or short dose treated mice were injected into NOD-SCID mice via tail vein. Fasting blood glucose levels (BGL) were measured at time of injection and monitored weekly after the adoptive transfer. Average BGL is shown for each group (n=2 mice per group). Figure completed in collaboration with Dr. Abby Dotson.

Discussion

LFA-1 and ICAM-1 play important roles in the development of autoimmune disorders (71). Current treatments targeting these two molecules center around antibody-based therapy, however given the immunogenic nature of antibodies, alternate therapies should be considered. Peptides were developed from the consensus binding sequences of both LFA-1 and ICAM-1 and were shown to be effective in blocking intercellular adhesion as well as inhibiting human T cell function within the context of a mixed lymphocyte reaction (72). Previous studies of the immunological effectiveness of these peptides in mediating rheumatoid arthritis were successful as well as a recent foray into type I diabetes. Data presented in this chapter show that treatment of NOD mice with only 7 injections ablates disease as compared to saline injected controls.

A long dose course of peptide treatment (17 injections) was effective in delaying the onset of disease as well as reducing insulitis, ablating antigenic recall and inducing death or anergy of auto-reactive T cells (73). The data accumulated throughout the course of both the long dose experiment and the short dose experiment presented in this chapter suggest that blocking the LFA-1/ICAM-1 interaction with peptides inhibits both T cell localization and function. Previous studies targeting LFA-1/ICAM-1 but conducted using monoclonal antibodies attributed the reduction of T1D symptoms to the inability of lymphocytes to enter islets (74). Our data suggest that the peptides inhibit not only the ability of self-reactive T cells to enter islets, but also inhibit T cell activation and function as demonstrated by the observation that T cells from treated mice could not respond to islet specific antigen in a recall response.

Previous studies by other investigators examined blocking specific costimulatory molecules in an attempt to inhibit various autoimmune diseases, including T1D. Use of a CTLA4Ig fusion protein to interfere with the B7/CD28 pathway proved successful in inhibiting disease when administered at 2-4 weeks of age in NOD mice, but was not effective after 10 weeks (75). This therapy also did not inhibit insulitis regardless of the age of the mice at initial treatment. Combination therapies targeting multiple costimulatory pathways have also not been proven to be any more effective than blockage of each individual pathway (76). It appears that blocking both T cell activation and migration into the islets is key to halting disease progression.

While the long dose treatment delayed the onset of diabetes as compared to the saline control, the peptide treated mice still did develop overt diabetes by the end of the study. Interestingly, it appears that decreasing the treatment regimen from 17 to 7 doses effectively inhibited the ability of the NOD mice to develop disease (**Figure 3.3**). Since the studies were not done concurrently, it is difficult to draw specific conclusions. The long dose study used larger groups of mice that could account for the differences seen between the treatment regimens. It is also possible that we have simply gotten better at conducting the experiments with the short dose. Still, while it is possible that the difference between studies could account for the differences in the development of disease, it is interesting to speculate that a shortened dose of peptide therapy may ablate disease completely while a longer dose simply results in a delay of onset. Future studies directly comparing both long and short dose treatments using large groups of mice would be able to shed light on this question and are planned for the future.

The data presented in this chapter show that using a shortened course of peptide treatment (7 injections) was as effective as a long dose treatment (17 injections) in ameliorating type I diabetes in a mouse model. The short dose treated groups showed improvement in both overt diabetes as seen in the consistently low blood glucose levels as well as on the cellular level as demonstrated by the reduction of lymphocyte infiltration into the islets. Future projects examining the kinetics of the short dose therapy as well as looking into the possibility of β-cell regeneration after the cessation of therapy are planned. Assessing the ability of the peptides to function in organ transplant rejection as well as other autoimmune disease models have also been proposed and will likely be completed in the future.

Chapter 4:

Development and evaluation of redesigned LFA-1 and ICAM-1 derived peptides using a computational approach

Introduction

As discussed previously, therapies that directly interfere with ICAM-1/LFA-1 binding have extensive therapeutic potential. While antibodies directed against these two molecules have shown promise, the deleterious effects associated with their use rarely outweigh the benefit. In an attempt to develop alternate methods of blocking the interaction, Dr. Scott Tibbetts developed short peptides targeted against each molecule. Each peptide was derived from the binding interface of LFA-1/ICAM-1 and tested for both toxicity and effectiveness. While the native derived peptides have shown tremendous promise in treating several autoimmune diseases and modulating the immune response, we sought to develop using a computational approach an alternate set of peptides that bound more tightly to the native protein. Several current therapeutics have been born from using a computational approach exploiting the protein-protein interactions between molecules to mediate disease. Recently, a structure-based design of an amyloid fibril inhibitor showed promise in disrupting fibril formation whose accumulation is associated with developing Alzheimer's disease (77). We hypothesized that this approach would enhance the efficacy of the peptides by allowing for a blockade of the ICAM-1/LFA-1 interaction that lasted longer than the native peptides thus enhancing the effectiveness of the therapy.

Rosetta is a software package developed to predict protein structure and function (79). The program samples conformational space associated with the input structures and evaluates the energy changes of the resulting model. The input structures are taken from the Protein Data Bank (PDB), which houses the experimentally mapped crystal structures

of proteins (80). Once the correct PDB accession number is given, the modeling program optimizes both the structure and sequence of the protein. Rosetta considers every amino acid at each position along the protein sequence and outputs an energy value, ΔΔg, for all variants. This ΔΔg value correlates to the stability difference between a mutated variant and the native, wild-type protein. A higher ΔΔg value therefore represents a protein variant that is less stable than its wild-type counterpart. Consequently, a negative ΔΔg value would indicate a more stable structure than the native protein. By using Rosetta, we were able to design alternate peptides that included two point mutations that were computationally predicted as being more stable than the native structure. We tested these "redesigned" peptides in *in vitro* assays of T cell adhesion and function to assay their behavior in relation to the native peptides.

Materials and Methods

Antibodies and reagents. Hybridomas expressing anti-CD54 (R6.5) and anti-CD11a (HB202) were purchased from ATCC (Manassas, VA) and antibodies were purified from serum-free medium using protein G affinity chromatography (Amersham). CD4-FITC was purchased from BioRad. Anti-CD3 (OKT3) stimulating antibody was purchased from BD Biosciences. Anti-CD28 (ANC28.1) was purchased from Ancell. Antibodies were used at a concentration of 5 μg/mL. MDHC (methyl-2,5-dihydroxycinnamate) was obtained from Toronto Research Chemicals and used at a concentration of 10 μM.

Cell purification and culture. Fresh human tonsil cells or peripheral blood were used for the activation experiments. Tonsils were minced in tissue culture PBS [137 mM NaCl, 2.7 mM KCL, 1.5 mM KH_2PO_4, 9.6 mM Na_2HPO_4, 0.7 mM CaCl, 0.5 mM $MgCl_2$, 10 mM glucose] with 2% fetal bovine serum and pen/strep (50 U/mL each) and cells in suspension were separated from tissue using a strainer. Peripheral blood was diluted 1:1 in TC-PBS. Cell suspensions were layered 3:1 over Ficoll (Pharmacia) and centrifuged at 1800 rpm for 30 minutes. The mononuclear cell layer was then isolated and rinsed with TC-PBS. The T cells were then separated using the E-rosette method (81). Freshly isolated cells were rested overnight at 37°C prior to experimentation.

For tonsillar T cells, greater than 95% of T cell isolates were positive for the T cell surface marker CD3, as assessed by flow cytometry. For peripheral T cells, greater than 98% of T cell isolates were positive for CD3. Culture medium for fresh T cells and

Molt-3 was RPMI 1640 supplemented with 10% FBS, 50 U/mL each of pen/strep and L-glutamine (2 mM).

Redesigned peptides. Redesigned peptides were computationally prepared using Rosetta's specificity switch code. The LFA-1/ICAM-1 crystral structure (PDB accession # 1MQ8) was used as the input structure. Each resulting variant and the associated free energy change was stored and only those variants located within the binding interface (residues 26-35 on ICAM-1 and residues 237-246 on LFA-1, correlating to the native peptide sequence location) were considered (**Figure 4.1**). Of the mutations within those sequences, the predicted structure with the mutation having the lowest ΔΔg value was run through the specificity switch program again to obtain a second stabilizing mutation by again choosing the mutation with the lowest associated ΔΔg value. From the predicted and calculated structures, the redesigned peptides were constructed (**Table 3**). The predicted structure of the LFA-1-derived redesigned peptide (rcLAB-L) is shown in **Figure 4.2** and the predicted structure of the ICAM-1-derived redesigned peptide (rcIE-L) is shown in **Figure 4.3**.

Cyclized redesigned peptides were purchased from American Peptide Company. Lyophilized peptides were stored desiccated at -20^{o}C until use at which time they were resuspended in culture medium at the indicated concentrations.

Homotypic adhesion assay. For antibody-stimulated samples, 96-well plates were coated with anti-CD3 for 3 hours at 37 ^{o}C and washed extensively with PBS to remove any unbound antibody. Molt-3 T cells were then added to the plate at a concentration of 10^5

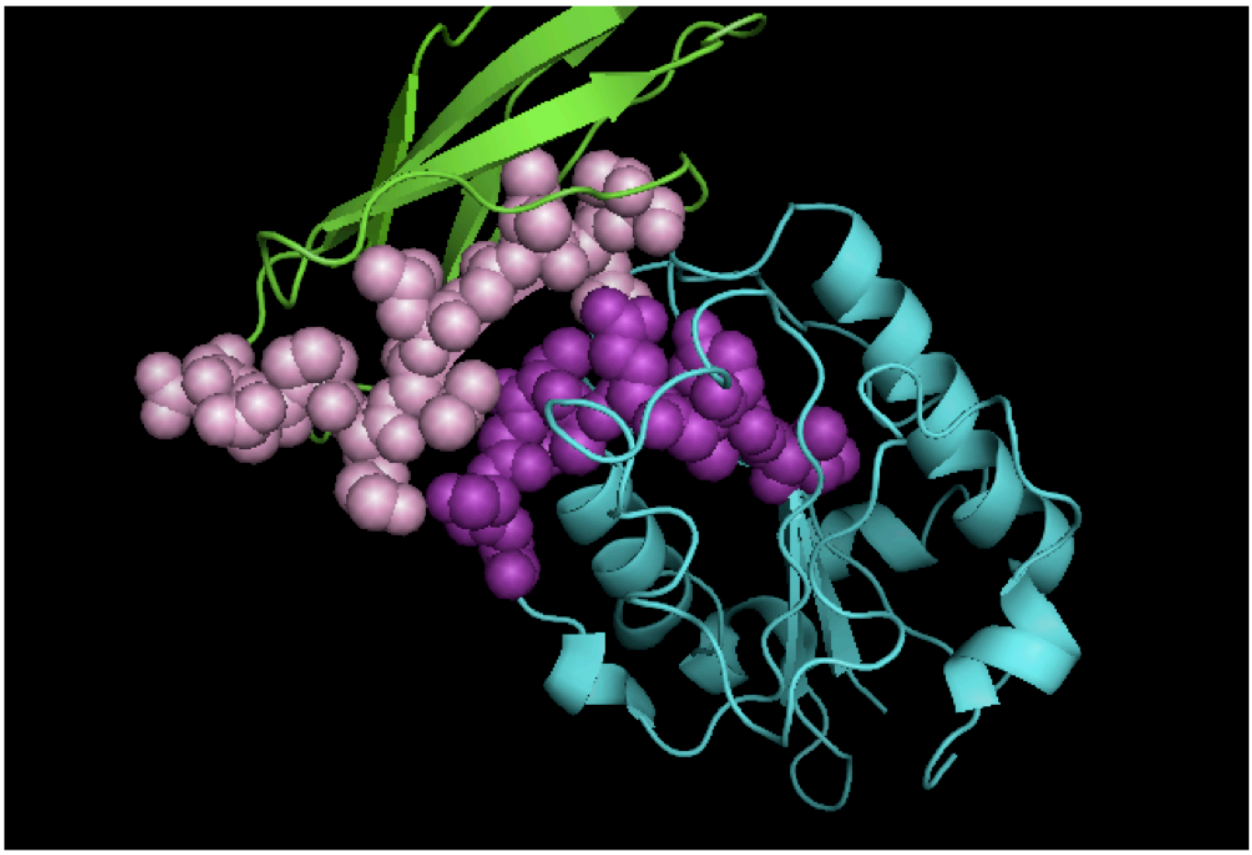

Figure 4.1. The binding interface between LFA-1 and ICAM-1
A rendition of the crystal structure of LFA-1α in complex with ICAM-1 (Uniprot ID: 1MQ8) created in PyMol. The green protein structure is LFA-1α with the LFA-1α binding domain highlighted in pink (LAB-L peptide). The aqua protein structure is ICAM-1 with the ICAM-1 binding domain highlighted in purple (IE-L peptide).

Table 3

Interaction stabilizing peptides derived from LFA-1 and ICAM-1

Peptide	Original Sequence	Optimized Sequence	Source	Mutation	ΔΔg
rcLAB-L	DQPKLLGIET	DQPKLLVRET	LFA-1α	G32V	-105.38
				I33R	-0.9
rcIE-L	ITDGEATDSG	IHDGEATDWG	ICAM-1	S245W	-0.57
				T238H	-9.1

Figure 4.2. Structure of the redesigned LFA-1α peptide, rcLAB-L
A rendition of the crystal structure of LFA-1α in complex with ICAM-1 (Uniprot ID: 1MQ8) created in PyMol. The green protein structure is LFA-1α with the LFA-1α binding domain highlighted in pink (original LAB-L peptide). The residue highlighted in yellow corresponds to the G32V mutation and the residue highlighted in orange corresponds to the I33R mutation. The aqua protein structure is ICAM-1 with the ICAM-1 binding domain highlighted in purple (IE-L peptide).

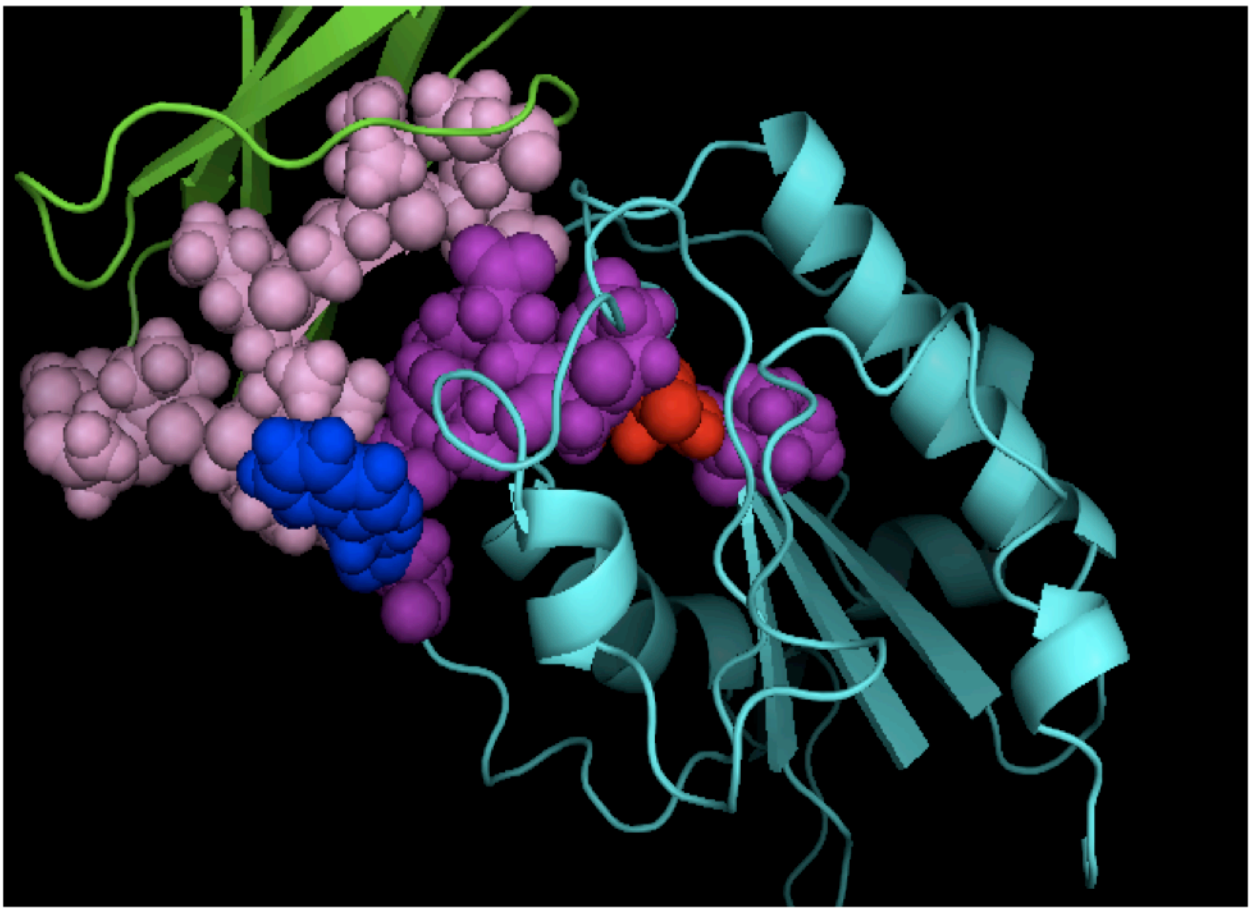

Figure 4.3. Structure of the redesigned ICAM-1 peptide, rcIE-L
A rendition of the crystal structure of LFA-1α in complex with ICAM-1 (Uniprot ID: 1MQ8) created in PyMol. The green protein structure is LFA-1α with the LFA-1α binding domain highlighted in pink (LAB-L peptide). The aqua protein structure is ICAM-1 with the ICAM-1 binding domain highlighted in purple (IE-L peptide). The residue highlighted in blue corresponds to the T243W mutation and the residue highlighted in red corresponds to the E241W mutation.

cells/well for 6 hours alone, with MHDC, or with MDHC plus varying concentrations of peptides. For analysis, three random fields of each sample were photographed at 40X magnification. The number of clumped cells was indirectly estimated as follows. The number of non-clumped cells in the nontreated plates was used as the baseline value. The number of clumped cells in the treated samples was approximated by counting the nonclumped cells in each of the fields and subtracting that number from the mean number of cells per field in the nontreated control.

Proliferation assay. Antibodies were attached to plastic by incubation for 3 hours at 37 ^{o}C and washed extensively with PBS to remove any unbound antibody. Fresh human T cells were stained with CFSE and plated at a concentration of 2 x 10^{6} cells/mL in the absence or presence of 250 μM of peptide. Cells were incubated for 3 days at 37 ^{o}C, harvested and proliferation quantified by flow cytometry.

Results

Both redesigned peptides inhibit MDHC-induced homotypic adhesion. LFA-1/ICAM-1-dependent homotypic adhesion of T cells is a reliable way for screening the ability of a compound to interfere with the interaction between LFA-1 and ICAM-1. As discussed in Chapter 1, our lab previously has published that the tyrosine kinase inhibitor MDHC can induce homotypic adhesion of Molt-3 cells and that this adhesion is a direct result of the ICAM-1/LFA-1 interaction (82).

As shown in **Figure 4.4**, both peptides were capable of inhibiting MDHC-induced homotypic adhesion. In **Panel B**, treatment of cells with MDHC resulted in the ability of the cells to form large aggregates of between 5 and 50 cells throughout the culture. In **Panel C**, treatment with rcIE-L at the same time as MDHC inhibited the ability of the cells to form clumps completely, with no clumps of more than 3 cells observed throughout the culture. This suggests that rcIE-L is capable of binding to LFA-1 and preventing the ICAM-1/LFA-1 interaction. Treatment with rcLAB-L showed similar results (**Panel D**) indicating that it is capable of binding to ICAM-1 and preventing the ICAM-1/LFA-1 interaction also.

To quantify the ability of the peptides to inhibit adhesion, the number of clumped cells per field was indirectly estimated as described in the *Materials and Methods* section of this chapter. **Figure 4.5** shows that treatment with rcIE-L significantly reduced adhesion as compared to the MDHC-treated control. Treatment with rcLAB-L displayed similar results as shown in **Figure 4.6**.

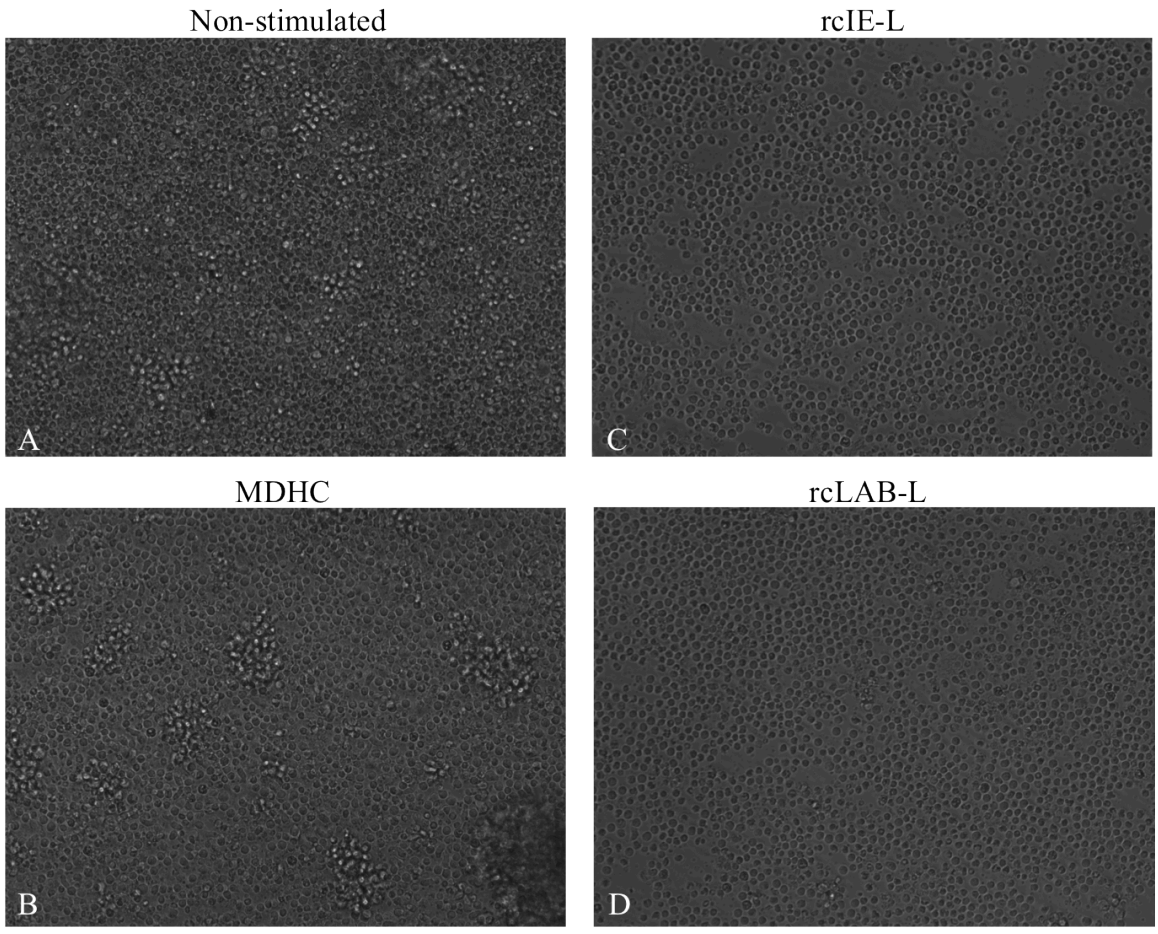
Non-stimulated
rcIE-L
A
C
MDHC
rcLAB-L
B
D

Figure 4.4. The redesigned peptides inhibit MDHC-induced LFA-1/ ICAM-dependent T cell homotypic adhesion
MOLT-3 T cells were left nonstimulated (*A*), stimulated with MDHC+ anti-CD3 to induce adhesion (*B*), or MDHC+anti-CD3 in the presence of 1 μM rcIE-L (*C*) or rcLAB-L (*D*). After incubation at 37°C for 6 hours, images were taken at 20X magnification.

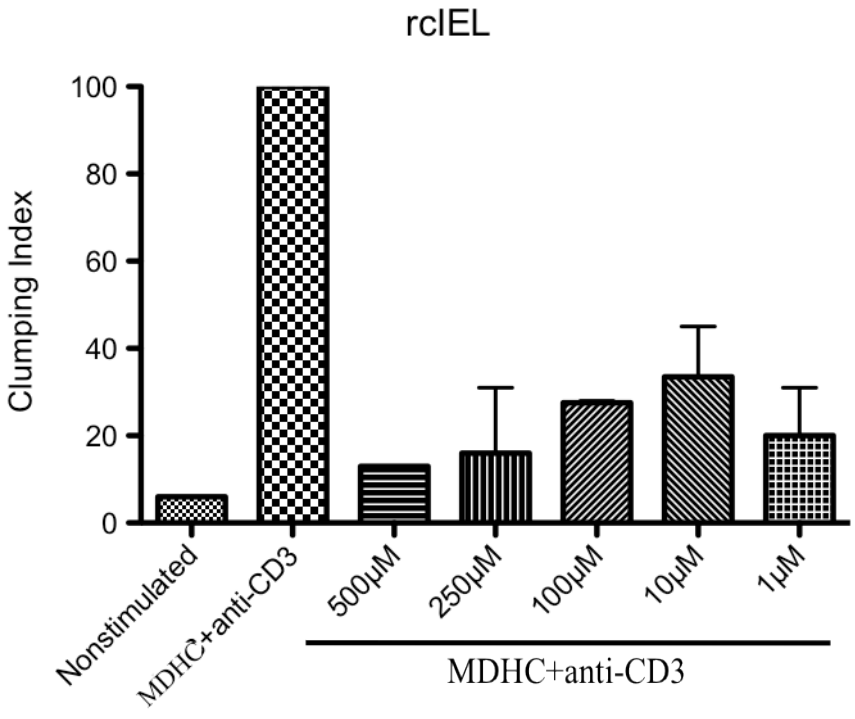
rclEL
Clumping Index
100
80
60
40
20
0
Nonstimulated
MDHC+anti-CD3
500μM
250μM
100μM
10μM
1μM
MDHC+anti-CD3

Figure 4.5. rcIE-L inhibited T cell homotypic adhesion and is dose-dependent

Peptide was tested at varying concentrations in the homotypic adhesion assay as described in *Materials and Methods*. Nonstimulated cells were used as a negative control and MDHC+anti-CD3 stimulated cells were used as a positive control for ICAM/LFA-1-dependent adhesion. Representative of three separate experiments. Y-axis values represent the mean clumping index.

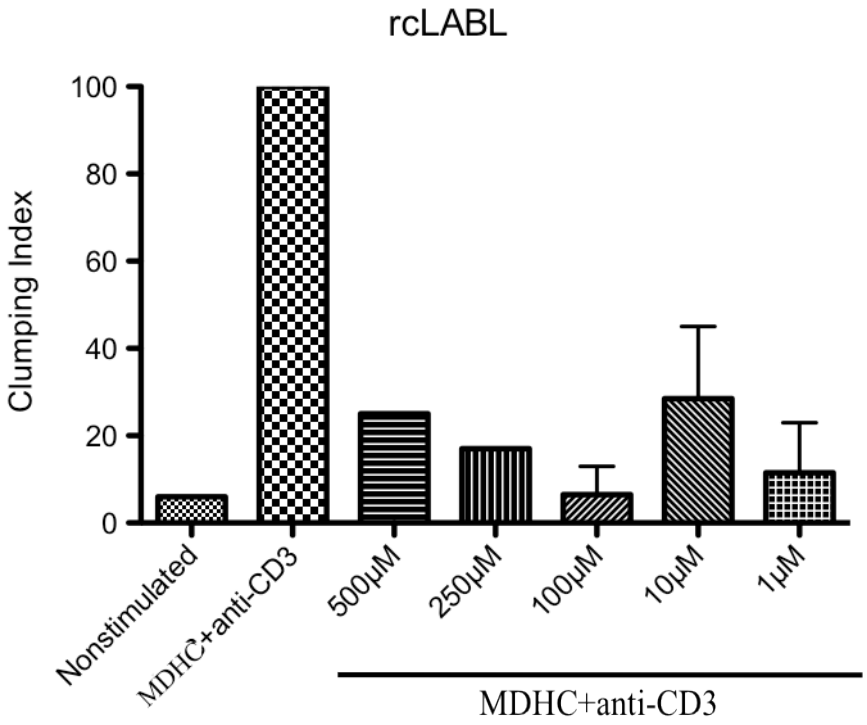
rcLABL
Clumping Index
100
80
60
40
20
0
Nonstimulated
MDHC+anti-CD3
500μM
250μM
100μM
10μM
1μM
MDHC+anti-CD3

Figure 4.6. rcLAB-L inhibited T cell homotypic adhesion and is not dose-dependent

Peptide was tested at varying concentrations in the homotypic adhesion assay as described in *Materials and Methods*. Nonstimulated cells were used as a negative control and MDHC+anti-CD3 stimulated cells were used as a positive control for ICAM/LFA-1-dependent adhesion. Representative of three separate experiments. Y-axis values represent the mean clumping index.

rcIE-L inhibition of homotypic adhesion is concentration-dependent. rcIE-L was tested at varying concentrations ranging from 1 μM up to 500 μM. As shown in **Figure 4.5**, treatment with rcIE-L significantly inhibited MDHC-induced adhesion in concentrations as low as 1 μM. An effective concentration of 24 μM has been previously reported using native peptides derived from ICAM-1, but the redesigned rcIE-L peptide was effective at inhibiting MDHC-induced adhesion in the lowest concentration tested of 1 μM (83).

rcLAB-L inhibition of homotypic adhesion is not concentration-dependent. rcLAB-L was tested at varying concentrations ranging from 1 μM up to 500 μM. Similar to the results seen with the ICAM-1 derived redesigned peptide, rcIE-L, treatment with the LFA-1 derived rcLAB-L significantly inhibited MDHC-induced adhesion in concentrations as low as 1 μM. However, the inhibition seen with rcLAB-L does not appear to be concentration dependent as illustrated in **Figure 4.6**. All concentrations tested were effective at inhibiting MDHC-induced adhesion.

rcIE-L enhances proliferation. We tested the effects of the redesigned rcIE-L peptide on T cell proliferation induced by anti-CD3. Stimulation through CD3 by the anti-CD3 antibody mimics the first signal through the T cell receptor that is required for T cell activation and proliferation. As a positive control, anti-ICAM-1 or anti-LFA-1 were added to anti-CD3 to mimic the second signal also required for full activation. The degree of proliferation was determined using CFSE staining. CFSE is taken up by the cells and partitioned equally as the cell divides. The resulting cell divisions can then be quantified by the amount of CFSE retained by using a flow cytometer. The proliferation

index correlates to the cells that have gone through one or more active cell divisions. As shown in **Figure 4.7**, co-culture of cells with rcIE-L enhanced T cell proliferation with stimulated with anti-CD3. Treatment with the alternative peptide did not significantly enhance proliferation when co-cultured with both anti-CD3 and either second signal-mimicking antibody.

rcLAB-L enhances proliferation. We also tested the effects of the redesigned rcLAB-L peptide on T cell proliferation by anti-CD3. As shown in **Figure 4.8**, co-culture of cells with rcLAB-L enhanced T cells proliferation with stimulated with anti-CD3 to a similar degree as both antibody second signals. Treatment with the alternative peptide did not significantly enhance proliferation when co-cultured with both anti-CD3 and either second signal-mimicking antibody similar to the results seen with rcIE-L.

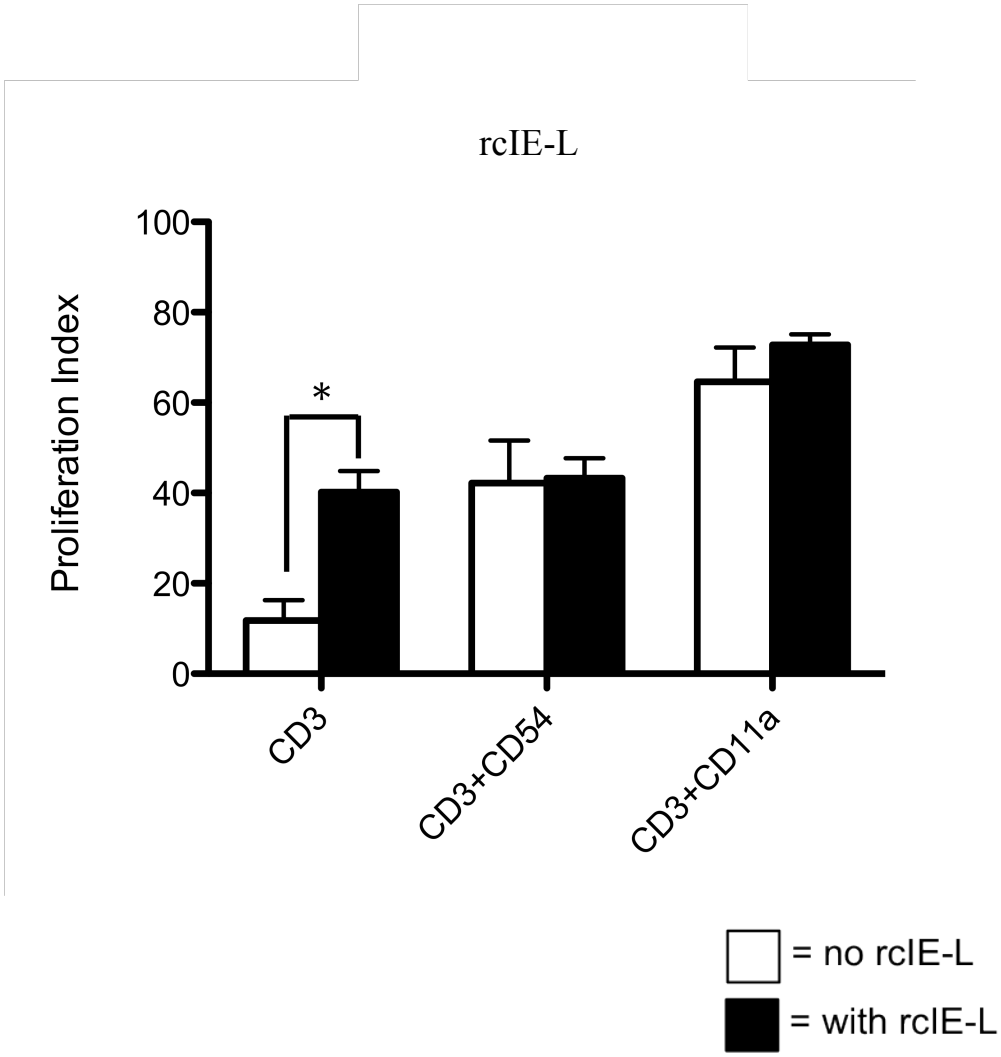
rcIE-L
Proliferation Index
100
80
60
40
20
0
*
CD3
CD3+CD54
CD3+CD11a
= no rcIE-L
= with rcIE-L

Figure 4.7. rcIE-L enhanced proliferation when cells were stimulated with anti-CD3

Human total T cells were stimulated with either anti-CD3 alone, anti-CD3+anti-CD54 or anti-CD3+anti-CD11a and incubated in the absence (white bars) or presence (black bars) of rcIE-L for 3 days. * = $p<0.05$. Representative of three separate experiments. Y-axis is the percentage of proliferating cells.

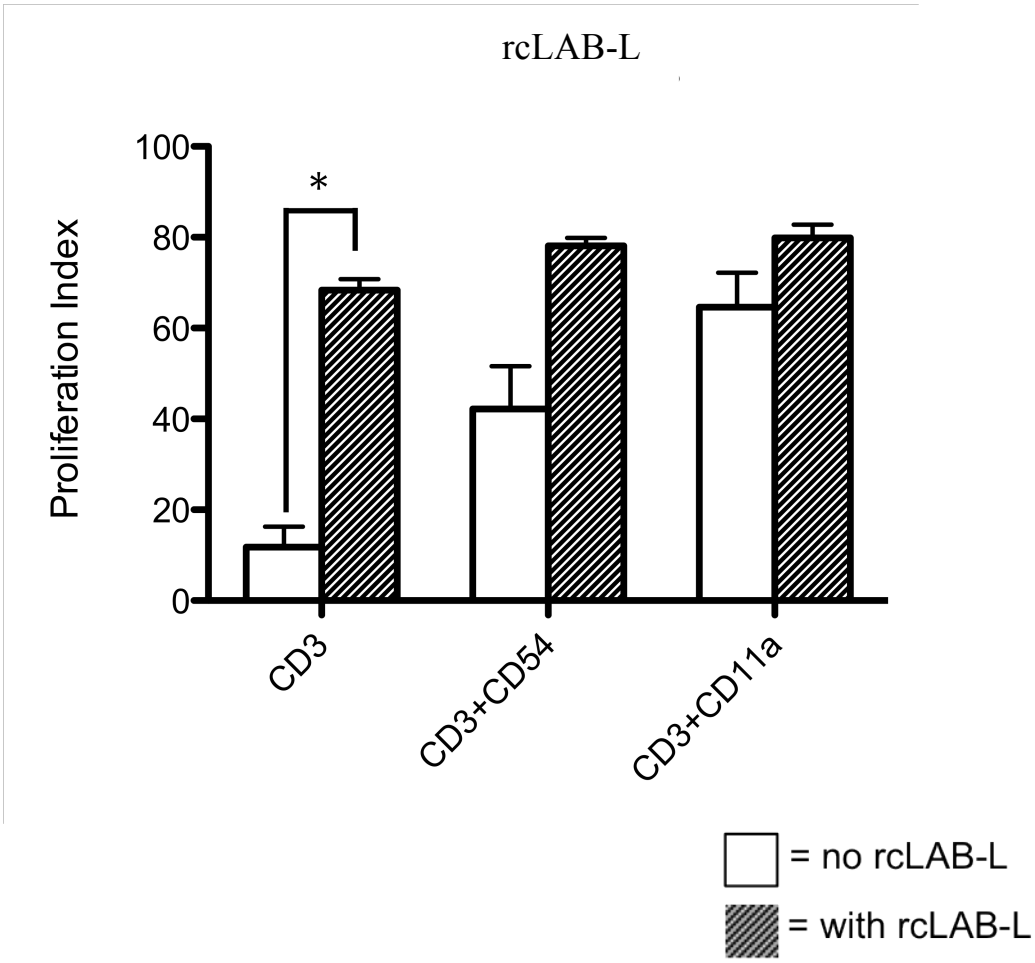
rcLAB-L
Proliferation Index
100
80
60
40
20
0
*
CD3
CD3+CD54
CD3+CD11a
= no rcLAB-L
= with rcLAB-L

Figure 4.8. rcLAB-L enhanced proliferation when cells were stimulated with anti-CD3

Human total T cells were stimulated with either anti-CD3 alone, anti-CD3+anti-CD54 or anti-CD3+anti-CD11a and incubated in the absence (white bars) or presence (black bars) of rcLAB-L for 3 days. * = $p<0.05$. Representative of three separate experiments. Y-axis is the percentage of proliferating cells.

Discussion

While the original goal of redesigning the peptides was to enhance the blockade between ICAM-1/LFA-1, we quickly learned that the redesigned peptides functioned in a different manner than the native peptides. Dr. Scott Tibbetts performed extensive experimentation on the native peptides, IE-L and LAB-L as well as others not located within the binding interface. The results from those experiments show that both the IE-L and LAB-L peptides were capable of inhibiting MDHC-induced T cell adhesion and were unable to stimulate T cell proliferation. It is hypothesized that the native peptides work by binding to the target site and physically blocking the interaction between ICAM-1 and LFA-1 from occurring. This blockage occurs without the peptide transducing a signal through it's target molecules, as would normally occur upon binding of the two full-length proteins.

When testing the redesigned peptides in some of the same assays Scott used, we ascertained that the redesigned peptides, rcIE-L and rcLAB-L, were also capable of inhibiting MDHC-induced adhesion as did their native counterparts. While both native peptides did so in a dose-dependent manner, only one of the redesigned peptides, rcIE-L behaved similarly. The LFA-1-derived rcLAB-L was capable of inhibiting MDHC-induced adhesion in all concentrations tested, but did not do so in a dose-dependent manner. Inhibition occurred at the same rate whether the cells were incubated with 500 μM or 1 μM of rcLAB-L. The differences in dose dependency may be explained by the binding states of the proteins. In order for tight binding of the adhesion molecules to occur, LFA-1 must be in the open, activated conformation (84). Because of the different

states of LFA-1, it is likely that higher concentrations of rcIE-L induce the conformation change from the low affinity state to the high affinity form of LFA-1. Conversely, the rcLAB-L peptide is likely mimicking the high-affinity, activated conformation of LFA-1 and therefore the peptide is effective at inhibiting adhesion at even very low concentrations. Regardless of the differences in dose-dependence between the redesigned peptides, we found that both rcIE-L and rcLAB-L were capable of inhibiting adhesion through ICAM-1/LFA-1.

Since both LFA-1 and ICAM-1 induce intracellular signaling in T cells as described in Chapter 1, we investigated the ability of the redesigned peptides to act as costimulatory molecules. The native peptides, when used alone or in conjunction with CD3 stimulation, were unable to induce proliferation in response to the peptide. This was attributed to the fact that the peptides likely have a lower affinity for the target protein than do the monoclonal antibodies. Since the redesigned peptides were predicted as having a higher affinity for the target protein, we would anticipate that they might also be able to transduce a signal and act as a costimulatory molecule themselves. To test this hypothesis, we performed proliferation assays. Human T cells were stimulated with anti-CD3 in the absence or presence of each peptide and proliferation assessed. As shown in Figures 24 and 25, both rcIE-L and rcLAB-L induced proliferation to the same level as the cells stimulated with monoclonal antibodies to LFA-1 and ICAM-1. This indicates that each redesigned peptide is capable of acting as a costimulatory molecule. While proliferation is a reliable index of T cell activation, further studies comparing cells costimulated with peptides and those using antibodies against ICAM-1 and LFA-1 should

be done to verify the signaling cascades turned on by the peptides are the same as those activated through antibody-mediated costimulation.

While the native peptides show promise for use in interventional therapies for autoimmune diseases, the redesigned peptides may be of use in preventative applications like vaccines. In addition to interventional therapies derived from using a computational approach, new advances in vaccine development have also arisen from the use of rational design. Vaccines require active T cell proliferation to occur in response to the target antigen being introduced. If the T cell response is correctly stimulated by the vaccine components, a memory response is generated to the target antigen. If the T cell response is not actively engaged, no proliferation occurs in response to the foreign antigen and immunity to the target antigen is not established thereby offering no benefit of the vaccine.

Peptide constructs have been developed as a vaccine delivery system that fuses a computationally optimized target epitope to a proprietary T cell epitope to activate a T cell response (78). This technology uses a computational approach to maximize the immune response to a foreign antigen by optimizing the antigen itself. This optimization includes introducing conformational restraint, if necessary, as well as fusion of the target antigen to a T cell-specific epitope. It is the fusion to the T cell-specific epitope that causes proliferation in response to the antigenic target. In contrast, we optimized T cell specific peptides and therefore do not require fusion to a T cell-specific epitope. This would allow for enhanced T cell activation that is requisite for a beneficial vaccine without changing the target antigen. By doing so, the redesigned peptides could be useful in vaccines that have a functional epitope mapped, but lack the intrinsic properties to

generate an active T cell response. Further testing assessing the toxicity and the effectiveness of the redesigned peptides in vaccine delivery needs to be completed using animal models. Since the native peptides were shown to not be toxic to cells, we would expect both rcIE-L and rcLAB-L to be nontoxic as well since the redesigned peptides share 80% homology, however toxicity still needs to be empirically tested.

The redesigned peptides might also be useful in individuals that are not capable of stimulating a T cell response to a vaccine such as those who are immunosuppressed or in the elderly population. Pilot studies using T cells harvested from elderly individuals (over age 65) showed that peptide treatment with either rcLAB-L or rcIE-L marginally enhanced T cell proliferation when also stimulated through CD3 (data not shown), however the cells did not stimulate well. Cells stimulated through CD3 and the monoclonal antibodies to ICAM-1 and LFA-1 did not proliferate above 20% so it is difficult to draw conclusions. Further studies into the effect of the redesigned peptides on the elderly population should be done to see their effectiveness on stimulating T cells that normally do not stimulate well.

References

1. Irving B, Weiss A. The cytoplasmic domain of the T cell receptor zeta chain is sufficient to couple to receptor-associated signal transduction pathways. *Cell*. 1991. 64: 891-901.

2. Letourneur F, Klausner R. Activation of T cells by a tyrosine kinase activation doamsin in the cytoplasmic tail of CD3 epsilon. *Science*. 1992. 255: 79-82.

3. Wolff H, Janeway C. Anti-CD45 augment response of a Th2 clone to TCR cross-linking. *Scand J Immunol*. 1994. 40: 22-25.

4. Oravecz T, Monstori E, Kurucz E, Takacs L, Ando I. CD3-induced T cell proliferation and interleukin-2 secretion is modulated by the CD45 antigen. *Scand J Immunol*. 1991. 34: 531-537.

5. Ledbetter J, Imboden J, Schieven G, Grosmaire L, Rabinovitch P, Lindsten T, Thompson C, June C. CD28 ligation in T cell activation: evidence for two signal transduction pathways. *Blood*. 1990. 75: 1531-1539.

6. Ceuppens J, Baroja M. Monoclonal antibodies to the CD5 antigen can provide the necessary second signal for activation of resting T cells by solid-phase-bound OKT3. *J Immunol*. 1986. 137: 1816-1821.

7. Bierer B, Peterson A, Gorga J, Herrmann S, Burakoff S. Synergistic T cell activation via the physiological ligands for CD2 and the T cell receptor. *J Exp Med*. 1998. 168: 1145-1156.

8. van Seventer G, Shimizu Y, Horgan K, Shaw S. The LFA-1 ligand ICAM-1 provides important costimulatoy signal for T cell receptor-mediated activation of resting T cells. *J Immunol.* 1990. 144: 4579-4586.

9. Fan S, Brian A, Lollo B, Mackman N, Shen N, Edington T. CD11a/CD18 (LFA-1) integrin engagement enhances biosynthesis of early cytokines by activated T cells. *Cell Immunol*. 1993. 148: 48-59.

10. Kohlmeier, J, Rumsey L, Chan M, Benedict S. The outcome of T cell costimulation through intercellular adhesion molecule-1 differs from costimulation through leukocyte function-associated antigen-1. *J Immunol.* 2003. 108: 152-157.

11. Chirathaworn C, Kohlmeier J, Tibbetts S, Rumsey L, Chan M, and Benedict S. Stimulation through intercellular adhesion molecule-1 provides a second signal for T cell activation. *J Immunol.* 2002. *168:*5330-53374

12. Kohlmeier J, Chan,M, and Benedict S. Costimulation of naïve human CD4+ T cells through ICAM-1 promotes differentiation to a memory phenotype that is not strictly the result of multiple rounds of cell division. *J Immunol.* 2006. 118:548-558.

13. Chirathaworn,C, Tibbetts S, Chan M, Benedict S. Cutting Edge: cross-linking of ICAM-1 on T cells induces transient tyrosine phosphorylation and inactivation of cdc2 kinase. *J Immunol.* 1995. 155:5479

14. Defilippi P, Gismondi A, Santoni A, Tarone G. Signal transduction by integrins. Landes Bioscience; Austin, TX. 1997.

15. Eble J, Kuhn K. Integrin-ligand interactions. Landes Bioscience; Austin, TX. 1997.

16. Hynes R. Integrins: bidirectional, allosteric signaling machines. *Cell*. 2002. 110: 673-687.

17. Kotovuori A, Pessa-Morikawa T, Kotovuori P, Nortamo P, Gahmberg C. ICAM-2 and a peptide from its binding domain are efficient activators of leukocyte adhesion and integrin affinity. *J Immunol*. 1999. 162 (11): 6613–6620.

18. Lu C, Takagi J, Springer T. Association of the membrane proximal regions of the alpha and beta subunit cytoplasmic domains constrains an integrin in the inactive state. *J Biol Chem*. 2002. 276 (18): 14642–14668.

19. Huang C, Springer T. A binding interface on the I domain of lymphocyte function-associated antigen-1 (LFA-1) required for specific interaction with intercellular adhesion molecule 1 (ICAM-1). *J Biol Chem*. 1995. 270 (32): 19008–19016

20. Wixler V, Geerts D, Laplantine E, Westhoff D, Smyth N, Aumailley M, Sonnenberg A, Paulsson M. The LIM-only protein DRAL/FHL2 binds to the cytoplasmic domain of several alpha and beta integrin chains and is recruited to adhesion complexes. *J Biol Chem*. 2000. 275 (43): 33669–33678.

21. Rietzler M, Bittner M, Kolanus W, Schuster A, Holzmann B. The human WD repeat protein WAIT-1 specifically interacts with the cytoplasmic tails of beta7-integrins. *J Biol Chem*. 1998. 273 (42): 27459–27466.

22. Binners M, van Kooyk Y, Simmons D, Figdor C. Distinct bnding of T lymphocytes to ICAM-1, -2 or -3 upon activation of LFA-1. *Eur J Immunol*. 1994. 24: 2155-2160.

23. van Kooyk Y, Weder P, Heije K, Figdor C. Extracellular Ca2+ modulates leukocyte function-associated antigen-1 cell surface distribution on T lymphocytes and consequently affects cell adhesion. *J Cell Biol*. 1994. 124: 1061-1070.

24. Dustin M and Springer T. T-cell receptor cross-linking transiently stimulates adhesiveness through LFA-1. *Nature*. 1989. 341: 619-624.

25. Campanero M, del Pozo M, Arroyo A. ICAM-3 interacts with and regulates the LFA-1/ICAM-1 cell adhesion pathway. *J Cell Biol.* 1993. 123: 1007-1016.

26. Lorentz H, Lagoo A, Hardy K. The cell and molecular basis of leukocyte common antigen (CD45)-triggered, lymphocyte function-associated antigen-1/intercellular adhesion molecule-1-dependent, leukocyte adhesion. *Blood.* 1994. 83: 1862-1870.

27. Cabanas C and Hogg N. Ligand intercellular adhesion molecule 1 has a necessary role in activation of integrin lymphocyte function-associated molecule 1. *Proc Natl Acad Sci.* 1993. 90: 5838-5842.

28. Pardi R, Bender J, Dettori C, Giannazza E and Engelman E. Heterogeneous distribution and transmembrane signaling properties of lymphocyte function-associated antigen (LFA-1) in human lymphocyte subsets. *J Immunol*. 1989. 143: 3157-3166.

29. Zheng J, Sjolander A, Eckerdal J, Andersson T. Antibody-induced engagement of β2 integrins on the adherent human neutrophils triggers activation of p21ras through tyrosine phosphorylation of the protooncogene product Vav. *Proc Natl Acad Sci.* 1996. 93: 8431-8436.

30. Fuortes M, Jin W, Nathan C. β2 integrin-dependent tyrosine phosphorylation of paxillin in human neutrophils treated with tumor necrosis factor. *J Cell Biol.* 1994. 127: 1477-1483.

31. Petruzzelli L, Takami M, Herrera R. Adhesion through the interaction of lymphocyte functin-associated antigen-1 and intercellular adhesion molecule-1 induces tyrosine phosphorylation of p130cas and its associated with c-CrkII. *J Biol Chem.* 1996. 271: 7796-7801.

32. Carrera A, Rincon M, Sanchez-Madrid F, Lopez-Botet M, de Landazuri M, Triggering of co-mitogenic signals in T cell proliferation by anti-LFA-1 (CD18/CD11a), LFA-3 and CD7 monoclonal antibodies. *J Immunol.* 1988. 141: 1919-1924.

33. Miller J, Knorr R, Ferrone M, Houdei R, Carron C, Dustin M. Intercellular adhesion molecule-1 dimerization and its consequence for adhesion mediated by lymphocyte function associated-1. J Exp Med. 1995. 44: 1661-1666.

34. de Fougerolles A, Klicksten L, Springer T. Cloning and expression of intercellular adhesion molecule 3 reveals strong homology to other immunoglobulin family counter-receptors for lymphocyte function-associated antigen-1. *J Exp Med.* 1993. 177: 1187-1192.

35. Van der Vieren M, Trong H, Wood C, Moore P, St. John T, Staunton D, Gallatin W. A novel leukointegrin, αdβ2, binds preferentially to ICAM-3. *Immunity.* 1995. 3: 683-690.

36. Hayflick J, Kilgannon P, Gallatin W. The intercellular adhesion molecule (ICAM) family of proteins. *Immunol Res.* 1998. 17: 313-327.

37. O'Toole T, Katagiri Y, Faull R. Integrin cytoplasmic domains mediate inside-out signal transduction. *J Cell Biol.* 1994. 124: 1047-1059.

38. O'Toole T, Ylanne J, Culley B. Regulation of integrin affinity states through an NPXY motif in the β subunit cytoplasmic domain. *J Biol Chem.* 1995. 270: 8553-8558.

39. Schaller M, Otey C, Hildebrand J, Parsons J. Focal adhesion kinase and paxillin bind to peptides mimicking β integrin cytoplasmic domains. *J Cell Biol.* 1995. 130: 1181-1187.

40. Kolanus W, Nagel W, Schiller B, Zeitlmann L, Godar S, Stockinger H, Seed B. αLβ2 integrin/LFA-1 binding to ICAM-1 induced by cytoadhesin-1, a cytoplasmic regulatory molecule. *Cell.* 1996. 86: 233-242.

41. Monks C, Freiberg B, Kupfer H, Sciaky N & Kupfer, A. Three-dimensional segregation of supramolecular activation clusters in T cells. *Nature.* 1998. 395: 82– 86.

42. Cherukuri A, Dykstra M, Pierce S. Floating the raft hypothesis: lipid rafts play a role in immune cell activation. *Immunity*. 2001. 14: 657–660.

43. Viola A, Schroeder S, Sakakibara Y, Lanzavecchia A. T lymphocyte costimulation mediated by reorganization of membrane microdomains. *Science.* 1999. 283: 680 – 682.

44. Xavier R, Brennen T, Li Q, McCormack C, Seed B. Membrane compartmentation is required for efficient T cell activation. *Immunity*. 1998. 8: 723-732.

45. Jackman JK, Motto DG, Sun Q, Tanemoto M, Turck CW, Peltz GA, et al.: Molecular cloning of SLP-76, a 76-kDa tyrosine phosphoprotein associated with Grb2 in T cells. *J Biol Chem.* 1995. 270: 7029-7032.

46. Bustelo X, Ledbetter J, Barbacid M. Product of vav proto- oncogene defines a new class of tyrosine protein kinase substrates. *Nature.* 1992. 356: 68-71.

47. Nel A, Gupta S, Lee L, Ledbetter J, Kanner S. Ligation of the T-cell antigen receptor (TCR) induces association of hSos1, ZAP-70, phospholipase C-gamma 1, and other phosphoproteins with Grb2 and the zeta-chain of the TCR. *J Biol Chem.* 1995. 270: 18428-18436.

48. Liu S, McGlade C. Gads is a novel SH2 and SH3 domain- containing adaptor protein that binds to tyrosine-phosphorylated Shc. *Oncogene.* 1998, 17: 3073-3082.

49. Reif K, Buday L, Downward J, Cantrell DA. SH3 domains of the adapter molecule Grb2 complex with two proteins in T cells: the guanine nucleotide exchange protein Sos and a 75-kDa protein that is a substrate for T cell antigen receptor-activated tyrosine kinases. *J Biol Chem*. 1994. 269: 14081-14087.

50. Koretzky G. The role of Grb2-associated proteins in T-cell activation. *Immunol Today*. 1997. 18: 401-406.

51. Trub T, Frantz JD, Miyazaki M, Band H, Shoelson SE: The role of a lymphoid-restricted, Grb2-like SH3-SH2-SH3 protein in T cell receptor signaling. *J Biol Chem* 1997. 272: 894-902.

52. Liu S, Fang N, Koretzky G, McGlade C. The hematopoietic-specific adaptor protein gads functions in T-cell signaling via interactions with the SLP-76 and LAT adaptors. *Curr Biol*. 1999. 9: 67–75.

53. Van Seventer G, Bonvini E, Yamada H, Conti A, Stringfellow S, June C, Shaw S. Costimulation of T cell receptor/CD3-mediated activation of resting human CD4+ T cells by leukocyte function-associated antigen-1 ligand intercellular cell adhesion molecule-1 involves prolonged inositol phospholipid hydrolysis and sustained release of intracellular Ca2+ levels. *J Immunol*. 1992. 149: 3872-3880.

54. Kim, M., C. V. Carman, W. Yang, A. Salas, T. A. Springer. The primacy of affinity over clustering in regulation of adhesiveness of the integrin α_{L2}. *J Cell Biol*. 2004. 167: 1241-1253.

55. Kinashi T. Intracellular signalling controlling integrin activation in lymphocytes. *Nat Rev Immunol*. 2005. 5: 546-559.

56. Luo B, Springer T. Integrin structures and conformational signaling. *Curr Opin Cell Biol*. 2006. 18: 579-586.

57. Graf B, Bushnell T, Miller J. LFA-1 mediated T cell costimulation through increased localization of TCR/Class II complexes to the central supramolecular activation cluster and exclusion of CD45 from the immunological synapse. *J Immunol*. 2007. 179: 1616-1624.

58. Sieh M, Batzer A, Schlessinger J, Weiss A. "GRB2 and phospholipase C-gamma 1 associate with a 36- to 38-kilodalton phosphotyrosine protein after T-cell receptor stimulation". *Mol Cell Biol*. 1992. 14: 4435–4442.

59. Zhang, W. et al. Essential role of LAT in T cell development. *Immunity.* 1999. 10: 323–332.

60. Parikh K, Poppema S, Peppelenbosch M, Visser L. Extracellular ligation-dependent CD45RB enzymatic activity negatively regulates lipid raft signal transduction. *Blood*. 2009. 113: 594-603.

61. Bluestone J, Herold K, Eisenbarth G: Genetics, pathogenesis and clinical interventions in type 1 diabetes. *Nature.* 2010. 464: 1293-1300.

62. Makino S, Kunimoto K, Muraoka Y, Mizushima Y, Katagiri K, Tochino Y. Breeding of a non-obese, diabetic strain of mice. *Jikken Dobutsu*. 1980. 29: 1-13.

63. Herold K, Gitelman S, Masharani U, Hagopian W, Bisikirska B, Donaldson D, Rother K, Diamond B, Harlan D, Bluestone J. "A single course of anti-CD3 monoclonal antibody hOKT3gamma1(Ala-Ala) results in improvement in C-peptide responses and clinical parameters for at least 2 years after onset of type 1 diabetes". *Diabetes.* 54: 1763–1769.

64. Kavanaugh A, Davis L, Nichols L, Norris S, Rothlein R, Scharschmidt L, Lipsky P. Treatment of refractory rheumatoid arthritis with a monoclonal antibody to intercellular adhesion molecule 1. *Arth Rheum.* 1994.37:992-999

65. Haug C, Colvin R, Delmonico F, Auchincloss H, Tolkoff-Rubin N, Preffer F, Rothlein R, Norris S, Scharschmidt L, Cosimi A. A phase I trial of immunosuppression with anti-ICAM-1 (CD54) mAb in renal allograft recipients. *Transplantation.* 1993. 55: 766-772

66. Turgeon N, Avila J, Cano J, Hutchinson J, Badell I, Page A, Adams A, Sears M, Bowen P, Kirk A, Pearson T, Larsen C. Experience with a novel efalizumab-based immunosuppressive regimen to facilitate single donor islet cell transplantation. *Am J Transplant.* 2010. 10: 2082-2091.

67. Isobe M, Yagita H, Okumura K, Ihara A. Specific Acceptance of Cardiac Allograft After Treatment with Antibodies to ICAM-1 and LFA-1. *Science*. 1992. 255: 1125-1127.

68. Anderson M, Bluestone J. The NOD mouse: a model of immune dysregulation. *Ann Rev Immunol.* 2005. 23: 447-485.

69. Sensi M. Pozzilli P, Ventriglia L, Doniach I, Cudworth A. Histology of the islets of Langerhans following administration of human lymphocytes into athymic mice. *Clin Exp Immunol.* 1982. 49: 81-86.

70. Christianson S, Shultz L, Leiter E. Adoptive transfer of diabetes into immunodeficient NOD-scid/scid mice: Relative contributions of CD4+ and CD8+ T-cells from diabetic versus prediabetic NOD.NON-Thy-1a donors. *Diabetes.* 1993. 42: 44-55.

71. McMurray R. Adhesion molecule in autoimmune diseases. *Sem Arth Rheu*. 1996. 25: 215-233.

72. Tibbetts S, Seetharama Jois D, Siahaan T, Benedict S, Chan M. Linear and cyclic LFA-1 and ICAM-1 peptides inhibit T cell adhesion and function. *Peptides*. 2000. 21: 1161-1167

73. Dotson A, Novikova L, Stehno-Bittel L, Benedict S. Elimination of T cell reactivity to pancreatic β cells by peptide blockade of LFA-1:ICAM-1 interaction after onset of diabetes in the NOD mouse model. *In preparation*.

74. Herold KC, Vezys V, Gage A, Montag AG: Prevention of autoimmune diabetes by treatment with anti-LFA-1 and anti-ICAM-1 monoclonal antibodies. *Cell Immunol*. 1994. 157: 489-500

75. Lenschow D, Ho S, Sattar H, Rhee L, Gray G, Nabavi N, Herold K, Bluestone J. Differential effects of anti-B7-1 and anti-B7-2 monoclonal antibody treatment on the development of diabetes in the nonobese diabetic mouse. *J Exp Med.* 1995. 181: 1145-1155

76. Nanji S, Hancock W, Luo B, Schur C, Pawlick R, Zhu L, Anderson C, Shapiro A. Costimulation blockade of both inducible costimulator and CD40 ligand induces dominant tolerance to islet allografts and prevents spontaneous autoimmune diabetes in the NOD mouse. *Diabetes* 2006. 55: 27-33

77. Sievers S, Karanicolas J, Chang H, Zhao A, Jiang L, Zirafi O, Stevens J, Munch J, Baker D, Eisenberg D. Structure-based design of non-natural amino-acid inhibitors of amyloid fibril formation. *Nature*. 2011. 475: 96-100.

78. Wang C, Walfield A. Site-specific peptide vaccines for immunotherapy and immunization against chronic diseases, cancer, infectious diseases and for veterinary applications. *Vaccine*. 2005. 23: 2049-56.

79. Leaver-Fay A, Tyka M, Lewis SM, Lange OF, Thompson J, Jacak R, Kaufman K, Renfrew PD, Smith CA, Sheffler W, Davis IW, Cooper S, Treuille A, Mandell DJ, Richter F, Ban YE, Fleishman SJ, Corn JE, Kim DE, Lyskov S, Berrondo M, Mentzer S, Popović Z, Havranek JJ, Karanicolas J, Das R, Meiler J, Kortemme T, Gray JJ, Kuhlman B, Baker D, Bradley P. ROSETTA3: an object-oriented software suite for the simulation and design of macromolecules. *Methods Enzymol*. 2011. 487: 545-547.

80. Berman H, Battistuz T, Bhat T, Bluhm W, Bourne P, Burkhardt K, Feng Z, Gilliland G, Iype L, Jain S, Fagan P, Marvin J, Padilla D, Ravichandran V, Schneider B, Thanki N, Weissig H, Westbrook J, Zardecki C. (2002) The Protein Data Bank. *Acta Crystallogr.* D58, 899–907.

81. Weiner M, Bianco C, Nussenzweig V. Enhanced binding of neuraminidase-treated sheep erythrocytes to human T lymphocytes. *Blood*. 1973. 43: 939-946.

82. Butler Y, Tibbetts S, Chirathaworn C, Benedict S. Modulation of T cell morphology and induction of homotypic adhesion by a protein tyrosine kinase inhibitor. *Cell Immunol*. 1995. 162: 129-138.

83. Fecondo J, Kent S, Boyd A. Inhibition of intercellular adhesion molecule 1-dependent biological activities by a synthetic peptide analog. *Proc Natl Acad Sci*. 1991. 2879-2882.

84. Hynes R. Integrins: Versatility, modulation and signaling in cell adhesion. *Cell*. 1992. 69: 11-25.